

The Wave-Driven Ocean Circulation

JAMES C. MCWILLIAMS

Department of Atmospheric Sciences and Institute of Geophysics and Planetary Physics, University of California, Los Angeles, Los Angeles, California

JUAN M. RESTREPO

Department of Mathematics and Program in Applied Mathematics, The University of Arizona, Tucson, Arizona

(Manuscript received 3 June 1998, in final form 4 November 1998)

ABSTRACT

Oceanic surface gravity waves have a mean Lagrangian motion, the Stokes drift. The dynamics of wind-driven, basin-scale oceanic currents in the presence of Stokes drift are modified by the addition of so-called vortex forces and wave-induced material advection, as well by wave-averaged effects in the surface boundary conditions for the dynamic pressure, sea level, and vertical velocity. Some theoretical analyses previously have been made for the gravity wave influences on boundary-layer motions, including the Ekman currents. The present paper extends this theory to the basin-scale, depth-integrated circulation in a bounded domain. It is shown that the Sverdrup circulation relation, with the meridional transport proportional to the curl of the surface wind stress, applies to Lagrangian transport, while the associated Eulerian transport is shown to have a component opposite to the Stokes-drift transport. A wave-induced correction to the relation between sea level and surface dynamic pressure is also derived. Preliminary assessments are made of the relative importance of these influences using a global wind climatology and an empirical relationship between the wind and wave fields. Recommendations are made for further development and testing of this theory and for its inclusion in general circulation models.

1. Introduction

The theory and simulation of persistent basin-scale oceanic currents, especially those near the surface where mariners travel and plankton grow, is a central problem in oceanography. It has long been understood that the prevailing surface winds are the primary driving mechanism for these currents, and in the first half of this century some simple models were developed to demonstrate this (e.g., Ekman 1905; Sverdrup 1947; Stommel 1948; Munk 1950). Subsequently, oceanic general circulation models (GCMs) have become much more sophisticated and geographically realistic [see the review in McWilliams (1996)]. Nevertheless, the quasi-steady, basin-scale patterns of both surface currents and depth-averaged (i.e., barotropic) horizontal mass transports given by GCMs have remained qualitatively similar to those predicted by the early simple models, in locations away from strong lateral boundary currents and their separation zones. The dynamical complications arising from other real-world influences—density

stratification, advective nonlinearity and turbulence, surface buoyancy fluxes, transient adjustment, bottom turbulent and form stresses, and basin geometrical complexity—all appear to be either quantitatively modest or dominant only on sub-basin scales or at great depths [for further discussion see Pedlosky (1996)]. There have been several empirical tests of the predicted relation between the wind stress and the depth-integrated transport on the basin scale in the equatorward flanks of the Northern Hemisphere subtropical gyres (e.g., Leetmaa et al. 1977; Hautala et al. 1994), and they showed an approximate consistency with the predictions of the simple theory [but note the caution expressed in Roemmich and Wunsch (1985) about the confidence we should place in such tests].

In the standard theory of ocean circulation, the turbulent boundary layer near the surface (i.e., the Ekman layer) responds to the surface wind stress with boundary-layer horizontal currents whose convergence causes a vertical divergence (i.e., Ekman pumping), which drives the interior, geostrophically balanced, horizontal circulation in extratropical oceanic gyres. The vertical integral of the total horizontal circulation is the Sverdrup transport. In this simple theory the sea state is ignored. However, surface gravity waves are capable of generating a mean Lagrangian current called the Stokes drift

Corresponding author address: Dr. James C. McWilliams, Dept. of Atmospheric Sciences, University of California, Los Angeles, 405 Hilgard Ave., Los Angeles, CA 90095-1565.
E-mail: jcm@atmos.ucla.edu

(Stokes 1847). The Stokes drift can affect the large-scale sea state in a sometimes dramatic way (e.g., Longuet-Higgins and Stewart 1960, 1961; Hasselmann 1971). It also influences the ocean currents. Hasselmann (1970) shows that the Stokes drift is capable of inducing, through the Coriolis force, both an opposing mean Eulerian current as well as inertial oscillations. Craik and Leibovich (1976, hereafter referred to as CL) show that the interaction of the Stokes drift with the mean flow could give rise to Langmuir circulation cells. Huang (1979) extends the CL model to include a spatially uniform Coriolis frequency. Webber (1983) and Webber and Melsom (1993) analyze the transfer of momentum to the Ekman layer due to wind and waves, including the effects of wave breaking in a simplified way; their solutions suggest that the wave-induced current and the Ekman current at the surface could be of the same magnitude. McWilliams et al. (1997) show how the results of CL and Huang have counterparts in the presence of turbulent boundary-layer dynamics. All of these studies suggest that, on the large horizontal scale of wind and wave variations and boundary-layer convergences, there may also exist surface gravity wave influences on the Sverdrup transport and on other properties of the basin-scale circulation. This possibility is the subject of this paper.

How can this possibility be investigated? With current technology direct numerical simulation is an impractical approach, since the range of time and space scales is extremely large, ranging from temporal $\Delta t \sim 10$ s and horizontal $\Delta x \sim 10\text{--}100$ m, for the dominant gravity waves, to $\Delta t \sim 10^8$ s and $\Delta x \sim 10^7$ m for the basin-scale circulations. To make the problem feasible, we pose it, at least conceptually, as a multiple-scale asymptotic expansion, where successive averages are made over “fast” motions to obtain appropriately filtered dynamic equations for the residual, or “slow,” motions. In the present instance there are three stages of averaging. The fastest component is the surface gravity waves, with scale content $\Delta t \sim 10$ s, $\Delta x \sim 10\text{--}10^2$ m, and vertical $\Delta z \sim 10\text{--}10^2$ m. A first average is taken in time or wave phase, yielding a residual Stokes-drift circulation. The next fastest component is the boundary-layer turbulence, with scale content $\Delta t \sim 10^3$ s, $\Delta x \sim 10\text{--}10^2$ m, and $\Delta z \sim 10\text{--}10^2$ m. A second average is made in time or horizontal coordinate over the turbulent eddies, yielding a residual Ekman boundary-layer current. Finally, a third average is made in time and horizontal (and perhaps vertical) coordinates, over meso-scale currents, with scale content $\Delta t \sim 10^6\text{--}10^7$ s, $\Delta x \sim 10^5\text{--}10^6$ m, and $\Delta z \sim 10^3$ m. This yields the slowest component, the general circulation with a Sverdrup transport driven by basin-scale variations in the winds and waves on seasonal timescales and longer.

To make progress, therefore, it is necessary to develop at least some parts of a multiple-scale theory, averaging over the surface gravity waves and relying on their dynamical simplicity at leading order in an expansion in

the wave slope. The template for this theory is the procedure outlined in CL, where the original interest was to explain near-surface, steady Langmuir cells by the interaction of surface waves with a wind-driven mean current, through the action of a “vortex force” proportional to the Stokes drift. Leibovich (1977a,b) extends the theory to allow a vertical density stratification and a slow-time variation [see Leibovich (1983) for a review of the dynamics of Langmuir circulation cells], and Huang (1979) derives a “Coriolis vortex force” in the wave-averaged Ekman-layer dynamics when the Coriolis vector can be taken as constant. We go several steps farther along this path with a CL-type theory for basin-scale circulation as our goal.

Specifically, we formulate a more complete theory for the wave-averaged dynamical effects of surface gravity waves. The modified Boussinesq equations we obtain are similar to those of Holm (1996), who uses a generalized Lagrangian mean (GLM) approach [Andrews and McIntyre (1978); also, Leibovich (1980), and Craik (1982) make GLM derivations of the original CL equations] within the formalism of Hamilton’s Principle to obtain hybrid Eulerian/Lagrangian equations for the slow-time dynamics of the Euler equations with rotation and stratification. As an application of the equations derived, we then present a new solution for the traditional simple models of the basin-scale circulation, including the effects of surface gravity waves through their Stokes-drift influences and the wave-averaged surface boundary conditions. The solution has the form of an ansatz based on the averaging hierarchy described above and empirical estimates for the wave field, rather than a more fundamental, explicit model for the slow part of the wave dynamics (which establishes the wave spectrum in response to wind forcing and dissipation). Obviously this is less than a complete theory, but it does indicate that the wave-driving may have some significant effects, ones that have previously been overlooked even in modern oceanic GCMs.

The perturbation theory is presented in section 2 for currents in the presence of surface gravity waves, where the latter are approximated to leading order by linear dynamics. In section 3 this theory is applied to the simple model for the large-scale oceanic circulation. In section 4 an empirical fit of the equilibrium gravity wave spectrum to the mean wind stress is used to estimate the climatological distributions of the relevant wave influences from wind data. Finally, section 5 presents our conclusions.

2. Wave-averaged dynamics

We analyze the dynamics in an oceanic region on the rotating earth containing a stratified, incompressible fluid, whose upper free surface is at $z = \eta(x, y, t)$ and whose rigid lower boundary is at $z = -D(x, y)$. The vertical coordinate is aligned antiparallel to the local gravitational force and is denoted by z ; $z = 0$ corre-

sponds to a quiescent ocean surface. On the free surface the pressure is equal to the atmospheric surface pressure. The position vector is denoted by $\mathbf{x} \equiv (\mathbf{x}_h, z)$, where the transverse or horizontal component is $\mathbf{x}_h = (x, y)$. Time is denoted by t . The Eulerian velocity is denoted by $\mathbf{q} \equiv (\mathbf{q}_h, w)$. The transverse component of differential operators and vector variables has a subscript h ; for example, $\nabla \equiv (\nabla_h, \partial/\partial z)$ and $D/Dt = \partial/\partial t + \mathbf{q}_h \cdot \nabla_h + w\partial/\partial z$. The oceanic dynamics are represented, as in CL and Leibovich (1977a,b), by the Boussinesq momentum and continuity equations,

$$\begin{aligned} \frac{\partial \mathbf{q}}{\partial t} + (\mathbf{q} \cdot \nabla)\mathbf{q} + \boldsymbol{\Omega} \times \mathbf{q} - \tilde{b}\hat{\mathbf{z}} + \frac{1}{\rho_0}\nabla\tilde{p} &= \nu\nabla^2\mathbf{q}, \\ \nabla \cdot \mathbf{q} &= 0, \end{aligned} \quad (1)$$

where ν is the viscosity, g is the gravitational acceleration, and ρ is the density, with ρ_0 its mean value. The unit vector $\hat{\mathbf{z}}$ is antiparallel to the gravitational force. The buoyancy field is defined by $\tilde{b} = g(1 - \rho/\rho_0)$, where the dynamic pressure, \tilde{p} , does not include the hydrostatic contribution $p_{\text{am}} - g\rho_0 z$ due to the mean atmospheric surface pressure, p_{am} , and the mean density of the resting ocean. The projection of the Coriolis vector, directed along the earth's axis of rotation, onto the local Cartesian coordinate system is $2\boldsymbol{\Omega} = [0, f^{(s)}(y), f^{(c)}(y)]$. Its spatial dependence is a consequence of variations of the local vertical direction with latitude. Since energetic, extratropical atmospheric and oceanic motions typically have large horizontal scales in comparison to the thickness of the fluid layer itself, it is usually possible to neglect the y component of the Coriolis vector.

We shall assume, for simplicity, that the buoyancy depends linearly on one or more passive tracers $\tilde{\theta}(\mathbf{x}_h, z, t)$, such as temperature or salinity, instead of the true nonlinear equation of state for seawater. The equation of state may thus be written as

$$\tilde{b} = g\Sigma_\theta\mu\tilde{\theta}, \quad (2)$$

where μ is the expansion coefficient for $\tilde{\theta}$ and Σ_θ denotes the sum over all the tracers that contribute to the buoyancy. In turn, the tracer dynamics are given by

$$\frac{D\tilde{\theta}}{Dt} = \kappa\nabla^2\tilde{\theta}, \quad (3)$$

where κ is the tracer diffusivity. We further assume that the tracer and buoyancy fields have a mean vertical stratification in the absence of any motion. Thus, we write the total buoyancy field as

$$\tilde{b} = \int^z N^2(z') dz' + b^*(\mathbf{x}, t), \quad (4)$$

where $N(z)$ is the Brunt-Väisälä frequency of the mean buoyancy stratification and b^* is the buoyancy deviation associated with fluid motions. Accompanying the mean stratification are each of the mean vertical tracer profiles $\Theta(z)$, so that

$$\tilde{\theta} = \Theta(z) + \theta^*(\mathbf{x}, t). \quad (5)$$

The pressure, \tilde{p} , is also assumed to have a mean $\Pi(z)$ and deviation p^* . The mean pressure is in hydrostatic balance with the mean stratification.

The surface boundary conditions at $z = \eta(\mathbf{x}_h, t)$ are the following:

$$\begin{aligned} w &= \frac{D\eta}{Dt}, & \tilde{p} &= g\rho_0\eta + \tilde{p}_a, \\ \nu\frac{\partial \mathbf{q}}{\partial z} &= \frac{1}{\rho_0}\boldsymbol{\tau}, & \kappa\frac{\partial \tilde{\theta}}{\partial z} &= \mathcal{T}. \end{aligned} \quad (6)$$

Here $\boldsymbol{\tau}$ and \mathcal{T} are the wind stress and surface tracer flux, respectively.

We are concerned with the situation whereby currents are influenced by surface gravity waves, characterized by an amplitude a and horizontal wavenumber with magnitude $k = |\mathbf{k}_h|$. We assume that the wave slope $\epsilon = ka$ is a small number and that $k|D| \gg 1$, so that these waves, to leading order, are approximately linear and uninfluenced by the ocean bottom. These assumptions lead to the deep-water dispersion relation $\sigma = \sqrt{gk}$, where σ is the frequency. The leading-order wave velocity field, $\mathbf{u}^w \equiv (\mathbf{u}_h^w, w^w)$, is irrotational (i.e., $\nabla \times \mathbf{u}^w = 0$), and it is assumed to be composed of a linear superposition of individual components with different horizontal wavenumbers, each of which has the solution form

$$\begin{aligned} \mathbf{u}_k^w &= -\nabla\varphi_k^w, \quad \text{with} \\ \varphi_k^w &= -\frac{e^{kz}}{k} \frac{\partial \eta_k^w(\mathbf{x}_h, t)}{\partial t}, \quad \text{and} \\ \eta_k^w &= a_k \cos[\mathbf{k}_h \cdot \mathbf{x}_h - \sigma_k t], \end{aligned} \quad (7)$$

where \mathbf{u}_k^w , φ_k^w , and η_k^w are the k th component of the velocity, velocity potential, and the free surface elevation, respectively. These gravity waves arise primarily through the interaction of the wind with the ocean surface. We will take their spectrum as given (see section 4) and ignore in this study the dynamics of their generation and dissipation. The dynamics of these waves, to leading order, are not influenced by the stratification; however, there is a wave-correlated component of the buoyancy and tracer fields, b^w and θ^w , due to the stratification. The leading-order, nondiffusive buoyancy balance and its resulting wave solution are

$$\begin{aligned} \frac{\partial b^w}{\partial t} &= -N^2(z)w^w \\ \Rightarrow b_k^w &= -a_k N^2(z)e^{kz} \cos[\mathbf{k}_h \cdot \mathbf{x}_h - \sigma_k t], \end{aligned} \quad (8)$$

with analogous relations for θ^w .

We nondimensionalize (1)–(6) by characteristic wave-propagation scales, that is, by the timescale $1/\sigma_0$ and the space scale $1/k_0$. The corresponding velocity scale is σ_0/k_0 , the pressure scale is $\rho_0(\sigma_0/k_0)^2$, the buoyancy scale is $(\sigma_0^2/k_0)B_0$, and the tracer scale is

$$[\sigma_0^2/(k_0 g \mu)] B_0.$$

The surface elevation η is scaled by $1/k_0$. In addition, we designate the Coriolis scale by $\sigma_0 \Omega_0$, the Brunt-Väisälä scale by $\sigma_0 N_0$, the viscosity and tracer diffusivity scale by $(\sigma_0/k_0^2) \nu_0$, the wind stress scale by $\rho_0(\sigma_0/k_0)^2 \tau_0$, and the tracer-flux scale by $[\sigma_0^3/(k_0^2 g \mu)] \mathcal{T}_0$. The nondimensional values of the B_0 , Ω_0 , N_0 , ν_0 , τ_0 , and \mathcal{T}_0 will be chosen to preserve certain balances in the asymptotic theory.

The theory to be presented shows that surface gravity waves, with a much faster timescale than most ocean currents, influence the dynamics of these currents. However, the form of the theory is potentially much more general than the particular situation we shall develop it for. Its essential basis is the presence of a rapidly varying irrotational flow, with zero time mean on this rapid timescale, which then can influence the dynamics of a weaker solenoidal component of the flow. Thus, variants of the theory may also apply to other types of fast oscillations, such as shallow water and internal waves. The separation between the solenoidal and irrotational components of the velocity field is in principle easily accomplished, formally or numerically, using the well-known Hodge (or Helmholtz) decomposition. Hence, the starting point for the theory is the following general form of the nondimensional velocity:

$$\mathbf{q} = \epsilon[\mathbf{u}^w(\mathbf{x}, t) + \delta \mathbf{v}(\mathbf{x}, t_s, t)], \quad (9)$$

where t is the fast time coordinate and $t_s = \gamma t$ is the slow time coordinate with $\gamma \equiv \epsilon \delta$. Here \mathbf{u}^w is assumed to be strictly irrotational, and \mathbf{v} contains the solenoidal component, with both fast- and slow-time dependencies. The parameter δ in (9), assumed small, will be specified later. To accompany (9), we write the nondimensional buoyancy and tracer fields as

$$b^* = \frac{B_0^w}{B_0} b^w(\mathbf{x}, t) + b(\mathbf{x}, t_s, t),$$

where $B_0^w = \epsilon N_0^2$ from (8), and

$$\theta^* = \frac{B_0^w}{B_0} \theta^w(\mathbf{x}, t) + \theta(\mathbf{x}, t_s, t). \quad (10)$$

The nondimensional vorticity equation comes from the curl of the momentum equation in (1):

$$\begin{aligned} \frac{\partial \boldsymbol{\omega}}{\partial t} + \gamma \frac{\partial \boldsymbol{\omega}}{\partial t_s} &= \frac{\Omega_0}{\epsilon \delta} \nabla \times [\epsilon(\mathbf{u}^w + \delta \mathbf{v}) \times 2\boldsymbol{\Omega}] + \nu_0 \nu \nabla^2 \boldsymbol{\omega} \\ &+ \nabla \times [\epsilon(\mathbf{u}^w + \delta \mathbf{v}) \times \boldsymbol{\omega}] \\ &+ \left(\frac{B_0}{\epsilon \delta}\right) \nabla \times \hat{\mathbf{z}} \left[b + \left(\frac{B_0^w}{B_0}\right) b^w \right], \end{aligned} \quad (11)$$

where

$$\boldsymbol{\omega} = \nabla \times \mathbf{v}.$$

Furthermore, after subtracting out the wave balance (8), the nondimensional buoyancy equation becomes

$$\begin{aligned} \frac{\partial b}{\partial t} + \gamma \frac{\partial b}{\partial t_s} + [\epsilon(\mathbf{u}^w + \delta \mathbf{v}) \cdot \nabla] \left[b + \left(\frac{B_0^w}{B_0}\right) b^w \right] + \left(\frac{N_0^2 \epsilon \delta}{B_0}\right) N^2 w \\ = \nu_0 \kappa \nabla^2 \left[b + \left(\frac{B_0^w}{B_0}\right) b^w \right]. \end{aligned} \quad (12)$$

The nondimensional form of (2) is $b = \Sigma_\theta \theta$. Thus, there are nondimensional tracer equations analogous to (12) for each of the component tracers.

We seek a general form for the asymptotic theory, which means that we formally choose values of the expansion parameters, which allow the various terms to all enter together at the leading nontrivial order in the governing equations for the evolution of $\boldsymbol{\omega}$ and b , on the slow timescale. The relations among the nondimensional parameters that allow this are the following:

$$\Omega_0, \nu_0, N_0 = O(\gamma); \quad B_0, \tau_0, \mathcal{T}_0 = O(\gamma^2). \quad (13)$$

Later we shall be more specific about the size of these parameters in the physical setting. Note that (13) implies that $B_0^w/B_0 = \epsilon$, and as a consequence, the wave-forced buoyancy fluctuations are of secondary importance in (11) and (12).

The vector and scalar field variables will be decomposed into mean and fluctuating components. The average of a quantity r , say, is defined by

$$\langle r(\cdot, t_s) \rangle = \frac{1}{T} \int_{t-T/2}^{t+T/2} r(\cdot, t_s, t') dt',$$

where T is the period of the gravity wave field. Hence, the t -average yields a quantity that varies in timescales typical of the longer wind and current variability. Application of these averages to the Eulerian velocity yields

$$\mathbf{v} = \langle \mathbf{v}(\mathbf{x}, t_s) \rangle + \mathbf{v}'(\mathbf{x}, t_s, t).$$

The model to be developed depends crucially on the assumptions that \mathbf{u}^w is periodic and that $\langle \mathbf{u}^w \rangle = 0$, as is true for the sinusoidal wave field described by (7).

The velocity and vorticity are expanded in ϵ ,

$$\mathbf{v} = \mathbf{v}_0 + \epsilon \mathbf{v}_1 + \epsilon^2 \mathbf{v}_2 + \dots,$$

and

$$\boldsymbol{\omega} = \boldsymbol{\omega}_0 + \epsilon \boldsymbol{\omega}_1 + \epsilon^2 \boldsymbol{\omega}_2 + \dots,$$

with analogous expressions for b and θ . When these are substituted in (11), we obtain a set of equations that are ordered by powers of ϵ . The lowest-order balance leads to

$$\boldsymbol{\omega}_0 = \boldsymbol{\omega}_0(\mathbf{x}, t_s).$$

After integration in t , the next-order balance gives a vorticity,

$$\boldsymbol{\omega}_1 = \nabla \times (\mathbf{U} \times \boldsymbol{\omega}_0) + \nabla \times (\mathbf{U} \times 2\boldsymbol{\Omega}), \quad (14)$$

where $\mathbf{U} \equiv \int^t \mathbf{u}^w(\mathbf{x}_h, s) ds$. Thus, $\langle \boldsymbol{\omega} \rangle = \boldsymbol{\omega}_0 + O(\epsilon)$ and $\boldsymbol{\omega}' = \epsilon \boldsymbol{\omega}_1 + O(\epsilon^2)$.

The t -average of (11) yields

$$\begin{aligned} \gamma \frac{\partial \boldsymbol{\omega}_0}{\partial t_s} = & \epsilon^2 \nabla \times \langle \mathbf{u}^w \times \boldsymbol{\omega}_1 \rangle + \gamma \nabla \times (\mathbf{v}_0 \times \boldsymbol{\omega}_0) + \gamma \nu \nabla^2 \boldsymbol{\omega}_0 \\ & + \gamma \nabla \times (\mathbf{v}_0 \times 2\boldsymbol{\Omega}) + \gamma \nabla \times (b_0 \hat{\mathbf{z}}), \end{aligned} \quad (15)$$

where we have used the relations in (13).

As shown in appendix A, the procedure described in CL enables us to derive the ‘‘vortex force,’’

$$\begin{aligned} \nabla \times \langle \mathbf{u}^w \times \boldsymbol{\omega}_1 \rangle = & (\boldsymbol{\omega}_0 + 2\boldsymbol{\Omega}) \cdot \nabla \mathbf{u}^s - \mathbf{u}^s \cdot \nabla (\boldsymbol{\omega}_0 + 2\boldsymbol{\Omega}) \\ = & \nabla \times [\mathbf{u}^s \times (\boldsymbol{\omega}_0 + 2\boldsymbol{\Omega})], \end{aligned} \quad (16)$$

where the quantity

$$\mathbf{u}^s = \left\langle \int^t \mathbf{u}^w(\mathbf{x}, s) ds \cdot \nabla \mathbf{u}^w \right\rangle \quad (17)$$

is the rescaled Stokes-drift velocity (i.e., with a dimensionalizing scale of $\epsilon^2 \sigma_0 / k_0$). Incorporating (16) into (15) and dividing by γ yields the equation for the leading-order, slow-time vorticity balance:

$$\frac{\partial \boldsymbol{\omega}_0}{\partial t_s} - \nabla \times [\mathbf{V} \times \mathbf{Z}] - \nabla \times b_0 \hat{\mathbf{z}} = \nu \nabla^2 \boldsymbol{\omega}_0, \quad (18)$$

where $\xi = \epsilon^2 / \gamma = \epsilon / \delta$ is a measure of the wave-added terms in these dynamics, $\mathbf{V} = \mathbf{v}_0 + \xi \mathbf{u}^s$, and $\mathbf{Z} = 2\boldsymbol{\Omega} + \boldsymbol{\omega}_0$. Equation (18) is similar to one derived in Holm (1996).

The curl operator can be made to operate explicitly on each term of the vorticity equation, which allows us to identify the compatible momentum equation. Since the divergence of the Stokes drift is zero and

$$-\nabla \times (\mathbf{v}_0 \times \boldsymbol{\omega}_0) = -\nabla \times \left[\nabla \left(\frac{|\mathbf{v}_0|^2}{2} \right) - \mathbf{v}_0 \cdot \nabla \mathbf{v}_0 \right],$$

we can express the momentum equation as

$$\frac{\partial \mathbf{v}_0}{\partial t_s} - \nabla \times \mathbf{Z} + \nabla \Phi - b_0 \hat{\mathbf{z}} = \nu \nabla^2 \mathbf{v}_0, \quad (19)$$

where we define

$$\Phi = p_0 + \frac{1}{2} \mathbf{V}^2 \quad (20)$$

as the nondimensional, generalized geopotential function. Since \mathbf{v}_0 is incompressible, the divergence of the momentum equation yields an elliptical problem for determining Φ :

$$\nabla^2 \Phi = \nabla \cdot (\mathbf{V} \times \mathbf{Z} + b_0 \hat{\mathbf{z}} + \nu \nabla^2 \mathbf{v}_0). \quad (21)$$

To obtain the boundary conditions for the slow-time vorticity and momentum balances, the boundary conditions (6) at the free surface $z = \eta^*$ are made nondimensional, analytically continued to the mean sea level $z = 0$ [i.e., $r(\eta^*) = r(0) + \eta^* \partial r / \partial z(0) + \dots$], expanded in wave and current components as above, and finally time averaged. The nondimensional surface elevation and pressure are assumed to have the forms

$$\begin{aligned} \eta^* = & \epsilon [\eta^w + \delta(\eta_0 + \epsilon \eta_1 \dots)], \\ p^* = & \epsilon [p^w + \delta(p_0 + \epsilon p_1 \dots)]. \end{aligned} \quad (22)$$

First we consider the kinematic condition in (6). Its leading-order, fast-time balance is the familiar wave condition, $w^w = \eta_t^w$. The time-averaged balance is

$$w_0 = \xi \nabla \cdot \mathbf{M} \quad \text{at } z = 0, \quad (23)$$

where

$$\mathbf{M} \equiv \langle \mathbf{u}^w(\mathbf{x}_h, 0, t) \eta^w(\mathbf{x}_h, t) \rangle. \quad (24)$$

In (23) we have used the fact that the term $\langle D\eta_0/Dt \rangle$ is smaller by $O(\gamma)$. On the other hand, if we were to assume that the horizontal variation of both the currents and wave statistics were on a slow scale $\mathbf{X}_h = \gamma \mathbf{x}_h$, then the amplitude of w_0 would be smaller by γ (for 3D continuity balance), and the boundary condition (23) would be generalized by the addition of $\partial \eta_0 / \partial t_s$ on the right-hand side. This addition would formally permit very long (i.e., shallow water) surface gravity waves in the current dynamics.

The nondimensional quantity \mathbf{M} represents the net mass flux per unit width associated with the waves. It is numerically equal to the mean wave momentum per unit area, $\langle \phi^w \nabla \eta^w \rangle$, to second order in ϵ , since the mean of the quantity $\nabla(\eta^w \phi^w)$ is zero when the flow is periodic both in space and time. The wave momentum term in the kinematic condition also appears in Hasselmann’s (1971) study of the interaction of long and short gravity waves. The pressure condition in (6) has the fast-time balance $p^w = \eta^w$ and the slow-time balance,

$$p_0 = \eta_0 + p_{a0} - \xi P \quad \text{at } z = 0, \quad (25)$$

where we have assumed that the slow atmospheric pressure variations p_{a0} scale in a similar way to p_0 , and the wave-added pressure adjustment term is

$$P \equiv \langle p_z^w(\mathbf{x}_h, 0, t) \eta^w(\mathbf{x}_h, t) \rangle = \langle (\eta_t^w)^2 \rangle = \langle (w^w)^2 \rangle, \quad (26)$$

with the second and third expressions obtained from the first one by using the linear balances that underlie the wave solution in (7). The stress condition in (6) is irrelevant to the leading-order wave dynamics because ν_0 is small in (13). The slow-time stress condition is

$$\nu \left(\frac{\partial \mathbf{v}_0}{\partial z} + \xi \mathbf{S} \right) = \tau \quad \text{at } z = 0, \quad (27)$$

where

$$\mathbf{S} \equiv \left\langle \frac{\partial^2 \mathbf{u}^w(\mathbf{x}_h, 0, t)}{\partial z^2} \boldsymbol{\eta}^w(\mathbf{x}_h, t) \right\rangle \quad (28)$$

is the wave-added correction.¹

Next we derive the slow-time tracer equation and thereby an equation for the evolution of the buoyancy. Leibovich (1977b) derives such an equation, albeit with an error later declared in Leibovich (1983). The tracer equation (3) is

$$\frac{\partial \theta}{\partial t} + \gamma \frac{\partial \theta}{\partial t_s} = -\epsilon(\mathbf{u}^w + \delta \mathbf{v}) \cdot \nabla \theta + \gamma \kappa \nabla^2 \theta, \quad (29)$$

as a consequence of (10), (12), and (13). Expanding

$$\theta = \theta_0 + \epsilon \theta_1 + \dots$$

and substituting into (29), the balance of terms leads to $\theta_0 = \theta_0(\mathbf{x}_h, z, t_s)$, to lowest order. Integration in time of the next-order balance yields

$$\theta_1 = -\mathbf{U} \cdot \nabla \theta_0, \quad (30)$$

which implies that $\langle \theta \rangle = \theta_0 + O(\epsilon)$ and $\theta' = \epsilon \theta_1 + O(\epsilon^2)$.

The t -average of (29) yields

$$\gamma \frac{\partial \theta_0}{\partial t_s} = -\epsilon^2 \langle \mathbf{u}^w \cdot \nabla \theta_1 \rangle - \gamma \mathbf{v}_0 \cdot \nabla \theta_0 + \gamma \kappa \nabla^2 \theta_0. \quad (31)$$

Substitution of (30) into the above equation and division by γ leads to the slow-time tracer equation (see appendix C):

$$\frac{\partial \theta_0}{\partial t_s} + \mathbf{V} \cdot \nabla \theta_0 = \kappa \nabla^2 \theta_0. \quad (32)$$

The tracer surface boundary condition (6) is particularly simple here: its fast-time expression is irrelevant to the wave dynamics because ν_0 is small, as in the stress condition above, and the wave-added terms in its slow-time form are negligible because $B_0^w/B_0 = \epsilon$. Thus, the slow-time boundary condition is the same as without surface waves,

$$\kappa \frac{\partial \theta_0}{\partial z} = \mathcal{T} \quad \text{at } z = 0. \quad (33)$$

We now summarize the model we have derived for the wave-averaged dynamics by reference to the pre-

¹ This truncated Taylor series expansion, while formally correct to leading order, neglects higher-order effects that arise due to the thin viscous boundary layer for waves whose thickness, $\sqrt{\nu/\sigma}$, is usually much smaller than $\langle \eta \rangle$ in the ocean. Here we are not concerned with its effects on the waves themselves, but there is a "mean streaming" contribution to the current dynamics from this wave boundary layer [e.g., see section 3.4 in Phillips (1977)], which a more relevant form of this boundary condition perhaps should incorporate. However, since viscous stress is so much smaller than turbulent Reynolds stress almost everywhere in the upper ocean, we do not here attempt to incorporate this type of correction in (27), since it is unlikely to be used in a circulation model anyway [e.g., see (33) below].

ceding nondimensional equations and surface boundary conditions to be applied at the mean sea level $z = 0$: momentum (19), vorticity (18), pressure (21), continuity ($\nabla \cdot \mathbf{v}_0 = 0$), tracer (32), surface velocity (23), surface pressure (25), surface stress (27), and surface tracer flux (33). Their dimensional counterparts are easily inferred by making the obvious reinterpretation of both the coordinates and variables and by dropping the expansion subscripts and the parameter ξ .

The equations thus derived have obvious parallels with the original Boussinesq system and the tracer equation if the velocity \mathbf{q} is replaced by \mathbf{V} , the sum of the lowest-order solenoidal velocity and the (steady) drift velocity, but with modified boundary conditions, which now preclude surface gravity wave solutions. Hence, many classical results with the rigid-lid approximation carry over to the wave-added dynamics. For example, the domain-integrated energy balance can be written in terms of \mathbf{V} as

$$\frac{d}{dt} \int \left[\frac{1}{2} \mathbf{V}^2 - z b_0 \right] d\mathbf{x} = - \int \left[\nu \nabla \mathbf{V} : \nabla \mathbf{v}_0 - \kappa \frac{\partial b_0}{\partial z} \right] d\mathbf{x},$$

when we assume that \mathbf{u}^s is time invariant and the boundary conditions are either periodic or have zero normal component for \mathbf{V} (fn2), and we neglect any boundary fluxes of momentum or buoyancy. Furthermore, by using the preceding vorticity and tracer equations, we can derive an expression for the potential vorticity balance, namely,

$$\frac{\partial Q}{\partial t} + \mathbf{V} \cdot \nabla Q = \nu \nabla b_0 \cdot \nabla^2 \boldsymbol{\omega}_0 + \kappa \mathbf{Z} \cdot \nabla (\nabla^2 b_0),$$

where the Ertel potential vorticity is defined as

$$Q = \mathbf{Z} \cdot \nabla b_0,$$

and contains no additional terms due to the wave averaging.

All effects arising from averaging over the wave motions appear multiplied by the parameter ξ . The wave-added terms in the momentum and tracer equations are proportional to the Stokes drift; they are the vortex force of CL, an analogous Coriolis vortex force, and a tracer advection. This latter effect may also be derived by comparing time-averaged Lagrangian and Eulerian representations of the motion of a passive tracer in which the velocity field is known, as in Longuet-Higgins (1953); in fact, the momentum equation can also be derived using Longuet-Higgins' prescription. These asymptotic theories can be contrasted to the GLM approach in which the drift terms are equivalent to the results given above only when the wave-induced dif-

² In particular, we have used $W = w_0 + w^s = 0$ at $z = 0$. This is derived from (23), the vertical integral of $\nabla \cdot \mathbf{u}^s = 0$, the assumption that \mathbf{u}^s at $z = -D$, and the identification of $\int_{-D}^0 \mathbf{u}^s dz$ with \mathbf{M} in (24) for the particular wave solution form (7); see section 3.

ference between the mean Lagrangian and Eulerian velocity fields is equal to the Stokes drift. In an asymptotic theory, one would have to go higher order to obtain a more accurate drift velocity expression than (17), whereas the GLM theory readily yields a general expression for the role of the drift. However, the GLM theory requires that the wave-induced displacement vector for the flow be known to make the model fully calculable. Beyond relying on asymptotic theories, such as the one here yielding the Stokes drift, we do not see how the wave-induced drift usually is determinable other than empirically or computationally (i.e., by tracking parcels in a known, time-averaged velocity field, with the necessary choices for the tracing and averaging times sometimes being difficult to justify).

We close this section with an evaluation of all the wave-added terms in the model above for a monochromatic wave solution (7), expressed in dimensional variables:

$$\begin{aligned} \mathbf{u}^s(z) &= \sigma k a^2 e^{2kz} \hat{\mathbf{k}}_h \\ \mathbf{M} &= \frac{1}{2} \sigma a^2 \hat{\mathbf{k}}_h \\ P &= \frac{1}{2} \sigma^2 a^2 \\ \mathbf{S} &= \frac{1}{2} \sigma k^2 a^2 \hat{\mathbf{k}}_h, \end{aligned} \quad (34)$$

where $\hat{\mathbf{k}}_h$ is the unit vector in the direction of the wave-vector \mathbf{k}_h . Magnitude estimates are made below in the context of the large-scale circulation.

3. Large-scale oceanic circulation

We now take a considerable step in spatial and temporal scales by making further approximations to the wave-averaged Boussinesq model of section 2 to obtain simpler equations appropriate for the large-scale oceanic general circulation. For this problem, we will continue to assume that the waves have the same leading-order, linear, irrotational dynamics as before, with the local (a, \mathbf{k}_h) spectrum determined by a higher-order dynamics obtained from either observations (as in section 4) or from a wave-dynamics model. The wave spectrum may be slowly varying in space and time on the scale of the general circulation, just as are the other external influences, the wind stress, and surface tracer fluxes. These slow variations of the wave field are superimposed on the local wave dynamics, which equilibrate on a shorter timescale.

The usual computational model for the general circulation, an oceanic GCM, is based upon the hydrostatic primitive equations (PE) with parameterizations for small-scale turbulent transport. However, experience justifies the further approximation to the planetary geostrophic equations (PG) where mesoscale eddy trans-

ports are parameterized and regions of narrow, intense currents are avoided (e.g., near the equator and the western boundaries). Because of their greater simplicity and robustness, we shall develop a PG model here, which includes wave-generated transport, rather than a more general PE variant. For simplicity, we shall assume an equation of state where density is conserved under adiabatic compression, and we shall use a local Cartesian coordinate system rather than the spherical coordinates of the earth's ocean. We shall defer until section 5 a discussion of the rather straightforward generalizations of these simplifying assumptions to the more fundamental PE equations that underlie modern GCMs.

To derive the PG equations, the following simplifications of the Boussinesq equations are made: 1) the vertical momentum equation is assumed to be in hydrostatic balance, 2) inertial terms and advective terms are ignored in the horizontal momentum equations (hence we also neglect the vortex force), and 3) the horizontal component of the Coriolis vector, $2\mathbf{\Omega}$, is neglected while the spatially variable vertical component, $2\Omega^{(z)}(y) \equiv f(y)$, is retained. As for any large-scale model, the PG equations include parameterized transports by smaller-scale motions not explicitly calculated in the model (e.g., eddy diffusion). This implies that our large-scale model results from yet another scale of averaging, beyond the wave scale used in section 2. It is interpreted as an average over small-scale turbulence, which is particularly strong in the top and bottom boundary layers, and over mesoscale eddies. Specifically, the average is an ensemble average, over independent realizations of these types of motion, so that it commutes with all other operators; in any comparison with nature, of course, a practical definition of the average as a space-time filter would be required.

With the preceding simplifications, the PG model equations in dimensional form are

$$\begin{aligned} f\hat{\mathbf{z}} \times \mathbf{v}_h &= -\nabla_h \phi - f\hat{\mathbf{z}} \times \mathbf{u}^s + \frac{\partial \mathbf{R}_v}{\partial z} + \nabla_h \cdot \mathbf{R}_h, \\ \phi_z &= b, \\ \nabla_h \cdot \mathbf{v}_h + w_z &= 0, \\ \frac{Db}{Dt} &= -\mathbf{u}^s \cdot \nabla_h b + \frac{\partial Q_v}{\partial z} + \nabla_h \cdot \mathbf{Q}_h. \end{aligned} \quad (35)$$

Here much of the notation is carried over from the previous section, where (\mathbf{v}_h, w) is the velocity, \mathbf{u}^s is the Stokes drift, b is the buoyancy, and $\phi \equiv p/\rho_0 \approx \Phi$ is the geopotential function in (20), and each of these quantities is wave and ensemble averaged. The approximation for ϕ is consistent with having neglected quadratic terms in the PG momentum balance. The quantities $(\mathbf{R}_h, \mathbf{R}_v)$ and (\mathbf{Q}_h, Q_v) represent, respectively, the (horizontal, vertical) momentum and buoyancy fluxes associated with smaller-scale motions and molecular diffusion:

$$\begin{aligned} \mathbf{R}_v &= -\overline{\mathbf{v}'_h w'} + \nu \frac{\partial \overline{\mathbf{v}}_h}{\partial z}, & \mathbf{R}_h &= -\overline{\mathbf{v}'_h \mathbf{v}'_h} + \nu \nabla \overline{\mathbf{v}}_h \\ Q_v &= -\overline{b' w'} + \kappa \frac{\partial \overline{b}}{\partial z}, & \mathbf{Q}_h &= -\overline{b' \mathbf{v}'_h} + \kappa \nabla \overline{b}. \end{aligned} \quad (36)$$

The overbar and prime symbols refer to ensemble averages and fluctuations. A complete specification of the PG model requires specification of the parameterization forms for the eddy fluxes in (36), but we shall not make these choices explicitly in the present paper.

We consider a bounded oceanic domain whose vertical extent is $-D(x, y) \leq z \leq \eta(x, y, t)$. The surface boundary conditions are linearized about $z = 0$ assuming small deviations $|\eta/D| \ll 1$; we take their forms from (23), (25), (27), and (33):

$$\begin{aligned} \phi - g\eta &= p_a/\rho_0 - P \\ w &= \nabla_h \cdot \mathbf{M} \\ \mathbf{R}_v &= \frac{1}{\rho_0} \boldsymbol{\tau}^t - \nu \mathbf{S} \approx \frac{1}{\rho_0} \boldsymbol{\tau}^t \\ Q_v &= \mathcal{B} \end{aligned} \quad (37)$$

at $z = 0$. The large-scale horizontal wind stress is $\boldsymbol{\tau}^t$ (where the superscript t denotes the top), and \mathcal{B} is the surface buoyancy flux. These boundary conditions are the wave-modified variants of the usual rigid-lid approximation for large-scale circulation, because we have neglected $\partial \eta / \partial t + \mathbf{v}_h \cdot \nabla \eta$ in the kinematic condition, consistent with the results in section 2. Note that the slow variations of the wave field are essential for a nontrivial wave-averaged effect in the kinematic condition: for a strictly monochromatic wave, \mathbf{M} has no spatial variation, hence zero divergence, whereas large-scale spatial variations of (a, \mathbf{k}_h) in (34) give a nonzero divergence. The approximation in the stress condition is based on the smallness of ν (about $10^{-6} \text{ m}^2 \text{ s}^{-1}$ for seawater). For any plausible wave conditions (e.g., with a dominant component with $a \sim 1 \text{ m}$, $k \sim 0.1 \text{ m}^{-1}$, hence $\sigma \sim 1 \text{ s}^{-1}$), we estimate $\nu \mathbf{S} \sim 10^{-8} \text{ m}^2 \text{ s}^{-2}$ to be very much smaller than $(1/\rho_0) \boldsymbol{\tau}^t \sim 10^{-4} \text{ m}^2 \text{ s}^{-2}$, with $|\mathbf{S}| \sim 10^{-2} \text{ s}^{-1}$ from (34).

The analogous conditions at the bottom boundary are

$$\begin{aligned} w &= -\mathbf{v}_h \cdot \nabla_h D \\ \mathbf{R}_v &= \frac{1}{\rho_0} \boldsymbol{\tau}^b \\ Q_v &= 0 \end{aligned} \quad (38)$$

at $z = -D$, where $\boldsymbol{\tau}^b$ is the bottom horizontal stress (which is also to be parameterized). Lateral boundary conditions are also required for (35) to be well posed.

For each vertical column, we can form a volume conservation law by integrating the continuity equation in (35) and using the kinematic vertical boundary conditions in (37) and (38):

$$\nabla_h \cdot \mathbf{T} = -\nabla_h \cdot \mathbf{M}, \quad (39)$$

where

$$\mathbf{T} \equiv \int_{-D}^0 \mathbf{v}_h dz \quad (40)$$

is the horizontal volume transport.

We form the vertical vorticity equation as the curl of the horizontal momentum equation in (35) and also use the continuity relation:

$$\begin{aligned} \beta v &= f w_z + \nabla_h \cdot (f \mathbf{u}^s) + \text{curl} \left[\frac{\partial \mathbf{R}_v}{\partial z} \right] \\ &+ \text{curl}[\nabla_h \cdot \mathbf{R}_h], \end{aligned} \quad (41)$$

where $\beta \equiv df/dy$. Vertically integrating (41), using the boundary conditions in (37) and (38), yields

$$\begin{aligned} \beta T^{(y)} &= -\beta T_{st}^{(y)} + \frac{1}{\rho_0} \text{curl}[\boldsymbol{\tau}^t - \boldsymbol{\tau}^b] + f \mathbf{v}_h^b \cdot \nabla_h D \\ &+ f \nabla_h \cdot [\mathbf{M} - \mathbf{T}_{st}] + \int_{-D}^0 \text{curl}[\mathbf{R}_h] dz, \end{aligned} \quad (42)$$

where \mathbf{T}_{st} is the horizontal transport of the Stokes drift,

$$\mathbf{T}_{st} \equiv \int_{-D}^0 \mathbf{u}^s dz, \quad (43)$$

and the superscripts t and b refer to top and bottom, respectively.

When we evaluate \mathbf{T}_{st} with a monochromatic linear wave solution (7), as in (34), we obtain

$$\mathbf{T}_{st} = \frac{1}{2} \sigma a^2 \hat{\mathbf{k}}_h. \quad (44)$$

Thus, $\mathbf{T}_{st} = \mathbf{M}$ for such a wave solution. This is not coincidental. After multiplication by ρ , (43) is an expression for the mean wave momentum. For irrotational periodic waves with zero Eulerian mean velocity, the only contribution to the mean momentum comes from the surface, whereas in the Lagrangian picture the mean momentum is the result of integrating distributed momentum throughout the fluid column, hence integrating the Stokes drift over the depth yields the mean wave momentum, in agreement with the result obtained in the Eulerian picture. Under the assumption that the irrotational flow is periodic in both space and time $\mathbf{T}_{st} = \mathbf{M}$, and the divergence term in the depth-integrated vorticity balance (42) cancels. However, this is not always the case, as, for example, if we allow for slow or large modulation of the irrotational wave field.

To further proceed with the analysis of (42), we make two additional simplifying assumptions: weak flow at depth, and weak eddy lateral momentum flux \mathbf{R}_h . The former simplification enables us to neglect the bottom stress and $\mathbf{v}_h^b \cdot \nabla_h D$ (this term contains the topographic pressure torque, or curl of the topographic form stress,

associated with the so-called JEBAR effect; see Pedlosky 1996). The latter simplification enables us to neglect the last term in (42). These two assumptions hold over most of the ocean, far away from its lateral boundaries, but they are not universally applicable. Incorporating these conditions and exploiting the numerical equivalence of \mathbf{M} and \mathbf{T}_{st} , we can replace (39) and (42), respectively, by

$$\nabla_h \cdot \mathbf{T} = -\nabla_h \cdot \mathbf{T}_{st} \quad (45)$$

and

$$\beta T^{(y)} = -\beta T_{st}^{(y)} + \text{curl} \left[\frac{1}{\rho_0} \boldsymbol{\tau}' \right]. \quad (46)$$

This comprises a closed set of equations for the horizontal transport \mathbf{T} , given $\boldsymbol{\tau}'$ and \mathbf{T}_{st} , which is a boundary-value problem in two space dimensions. It is easily solved in terms of a Lagrangian transport streamfunction $\Psi(x, y)$ defined by

$$\mathbf{T} + \mathbf{T}_{st} \equiv \hat{\mathbf{z}} \times \nabla_h \Psi. \quad (47)$$

From (46) the differential equation for Ψ is

$$\beta \Psi_x = \text{curl} \left[\frac{1}{\rho_0} \boldsymbol{\tau}' \right], \quad (48)$$

with an eastern-boundary condition of no normal transport,

$$\Psi = 0 \quad \text{at } x = X_{\text{east}}(y). \quad (49)$$

Note that (48)–(49) have the form of the usual Sverdrup transport relations, except that they refer here to the Lagrangian rather than Eulerian transport streamfunction; to obtain the latter, the Stokes transport must be subtracted from $\text{curl}[(1/\rho_0)\boldsymbol{\tau}']$.

Given the transport \mathbf{T} , we can solve separately for the complementary baroclinic fields. This is usually done as a nonlinear initial- and boundary-value problem in three space dimensions, because the evolutionary adjustment rates for b extend to timescales of millenia even with steady external forcing fields. The general procedure for the solution is to determine Φ , \mathbf{v}_h , and w given b , and then to step b forward in time. Whether the problem for \mathbf{T} is decoupled from the baroclinic problem depends largely on whether the final two approximations preceding (45) are made, since they both are usually associated with the baroclinic currents.

We can make a further boundary-layer approximation in the horizontal momentum balance in (35) when \mathbf{R}_v is small everywhere except in thin regions near the vertical boundaries. First, we decompose the horizontal velocity as

$$\mathbf{v}_h = \mathbf{v}'_{ek} + \mathbf{v}_{geo} + \mathbf{v}^b_{ek}. \quad (50)$$

The top and bottom Ekman velocities, \mathbf{v}'_{ek} and \mathbf{v}^b_{ek} , have a momentum balance in (35) between the left-hand side and the second and third right-hand side terms and also vanish into the vertical interior. Their vertical boundary

conditions are the middle two in (37) and the first two in (38) (with $\boldsymbol{\tau}^b$ a functional of \mathbf{v}_{geo} at $z = -D$). The geostrophic velocity, \mathbf{v}_{geo} , satisfies the remainder of (35). In each of these balances, it is customary to neglect the lateral eddy momentum flux in regions away from strong currents (as above).

With (50) we can integrate the Ekman balance in (35) over $-h'_{ek} \leq z \leq 0$, where h'_{ek} is the boundary-layer depth beyond which \mathbf{v}'_{ek} , \mathbf{u}^s , and \mathbf{R}_v are negligible:

$$\mathbf{T}'_{ek} = -\hat{\mathbf{z}} \times \frac{1}{f\rho_0} \boldsymbol{\tau}' - \mathbf{T}_{st}, \quad (51)$$

where

$$\mathbf{T}'_{ek} \equiv \int_{-h'_{ek}}^0 dz \mathbf{v}'_{ek}. \quad (52)$$

Thus, the Eulerian Ekman transport has a contribution that cancels the Lagrangian transport of the Stokes drift, as well as a component perpendicular to the wind stress; that is, the total Lagrangian transport in the boundary layer is perpendicular to the wind stress.

We now integrate the continuity relation over the boundary layer, neglecting any contribution from \mathbf{v}_{geo} :

$$\begin{aligned} w'_{ek} &= \nabla_h \cdot \mathbf{T}'_{ek} + \nabla_h \cdot \mathbf{M} = \text{curl} \left[\frac{1}{f\rho_0} \boldsymbol{\tau}' \right] + \nabla_h \cdot (\mathbf{M} - \mathbf{T}_{st}) \\ &= \text{curl} \left[\frac{1}{f\rho_0} \boldsymbol{\tau}' \right], \end{aligned} \quad (53)$$

where w'_{ek} is the Ekman pumping velocity at the base of the surface Ekman layer. The final expression in (53) is a consequence of $\mathbf{M} = \mathbf{T}_{st}$ for linear waves. Note that this implies that there is no wave-induced effect in w'_{ek} . Since Ekman pumping provides a significant forcing for \mathbf{v}_{geo} through the first term on the right-hand side of (41), the geostrophic flow in the interior therefore also lacks a direct wave-driven effect.

However, there is an indirect wave-driven effect on \mathbf{v}_{geo} through the dependence of Φ on b , which has advective influences from both \mathbf{v}_h and \mathbf{u}^s in the final equation in (35). The advecting velocity for tracers, $\mathbf{v} + \mathbf{u}^s$, has no wave-induced increment to the depth-averaged, wind-driven response in (46); furthermore, (51) shows that the Eulerian cancellation of the wave-induced transport occurs within the top boundary layer. Nevertheless, there is no reason to expect that the cancellation occurs pointwise, and the mechanisms of vertical momentum flux—Reynolds stress, \mathbf{R}_v , and isopycnal form stress, \mathbf{Q}_H and $\mathbf{v} \cdot \nabla b$ acting through the Coriolis force—determine how the wave-added advection is distributed with depth. McWilliams et al. (1997) shows that the Ekman-layer profile of $\mathbf{v}_h(z) + \mathbf{u}^s(z)$ in a large-eddy simulation (LES) solution is quite different from $\mathbf{v}_h(z)$ when wave driving is neglected.

We now make a simple assessment of the relative importance of the wave- and wind-driven effects based

on the Ekman transport relation (51). (This assessment will be made more elaborately in section 4.) A typical value for the wind-driven component is $(1/f\rho_0)\boldsymbol{\tau}' \sim 1 \text{ m}^2 \text{ s}^{-1}$, based on $f \sim 10^{-4} \text{ s}^{-1}$, $\rho_0 \sim 10^3 \text{ kg m}^{-3}$, and $\boldsymbol{\tau}' \sim 0.1 \text{ N m}^{-2}$. From (44), \mathbf{T}_{st} has the same magnitude for a monochromatic wave with amplitude $a = 1.34 \text{ m}$ and wavelength $2\pi/k = 50 \text{ m}$ (i.e., $k = 0.126 \text{ m}^{-1}$, $\sigma = 1.11 \text{ s}^{-1}$, and $\frac{1}{2}\sigma a^2 = 1 \text{ m}^2 \text{ s}^{-1}$), and neither of these a or k values is uncommon for ocean waves. Therefore, we conclude that the wave-driven effects sometimes are significant compared to the wind-driven ones.

This comparison can also be expressed with nondimensional parameters. We define \mathcal{R} as the ratio of the wind- and wave-driven components in (51),

$$\mathcal{R} \equiv \frac{|\boldsymbol{\tau}'/f\rho_0|}{|\mathbf{T}_{st}|}. \quad (54)$$

The turbulent Langmuir number,

$$\text{La}_{\text{tur}} \equiv \left(\frac{\sqrt{|\boldsymbol{\tau}'/f\rho_0|}}{|\mathbf{u}^s(0)|} \right)^{1/2}, \quad (55)$$

measures the relative influences of wind-driven shear instability and the Stokes-drift Coriolis force on the boundary-layer turbulence. Commonly observed values of La_{tur} are somewhat less than one (Smith 1992), and this range is also where the turbulent eddies begin to resemble Langmuir cells (McWilliams et al. 1997). We can therefore rewrite (54) as

$$\mathcal{R} = \text{La}_{\text{tur}}^2 \left(\frac{h_{\text{ek}}}{h_{st}} \right), \quad (56)$$

where $h_{\text{ek}} \equiv (\boldsymbol{\tau}'/f\rho_0)^{1/2}$ is the usual Ekman-layer depth and $h_{st} = 1/2k$ is the Stokes-layer thickness. Thus, we see a dependence of \mathcal{R} both on the relative strengths of the wind and waves and on the relative vertical length scales of the boundary-layer turbulence and the wave motions. Since the first right-hand-side factor here is typically smaller than 1 and the second is typically larger than 1, the two transport contributions can be comparable.

A few empirical tests of the Ekman transport relation (51) have been attempted directly from local current and wave measurements under the assumption that the Stokes drift can be calculated by (17) (Gnanadesikan and Weller 1995; Weller and Plueddemann 1996) have thus far failed to confirm (51), but the sampling uncertainties may have precluded a sufficiently discriminating test. This measurement strategy is a difficult one to carry out because of the time averaging and the dense and extensive vertical sampling needed in order to compute the vertical integrals for transports and to extract the approximate steady-state balance when the wind and wave statistics are stable in time. An alternative would be to make a pointwise test of the theory, which escapes the sampling burden of estimating transports; however, in this case, one would also have to deal with the in-

fluences of surface buoyancy forcing and stratification and turbulent fluxes, $\mathbf{R}_v(z)$ and $Q_v(z)$ in (36), in combination with $\mathbf{u}^s(z)$ in determining the vertical profiles of $v'_{\text{ek}}(z)$. Since the transport relation (51)—or its implicit pointwise balances—is a robust prediction of previous wave-averaged theories and ours, we believe it is very important to resolve the present apparent disagreement between theory and observations. We remark that our theory is not essentially tied to the Stokes drift only in the form given by (17). The fundamental relevant quantity is the wave-induced difference between the mean Lagrangian and Eulerian velocities, and experimental tests could attempt to measure this directly.

When the PG boundary-value problem is posed in the rigid-lid form above, then the surface pressure boundary condition in (37) can be used as a diagnostic relation for sea level, given $\phi(0)$ from the PG equation solution, since η otherwise drops out of the problem for ϕ , b , and the \mathbf{v} :

$$\eta = g^{-1}[\phi(0) - p_a/\rho_0 + P]. \quad (57)$$

The wave-induced effect here is not negligible compared to typical gyre-scale sea-level variations of a few tenths of a meter, since a monochromatic wave estimate (34) of P/g is 0.11 m for the same $(a, k) = (1.34 \text{ m}, 0.126 \text{ m}^{-1})$ values used above. More complete estimates of P are made in section 4.

Alternatively, (57) can be viewed, as it is in the interpretation of altimetric measurements, as a diagnostic relation for the surface geopotential field after correcting $g\eta$ for the inverse-barometric response by adding p_a/ρ_0 ; then $\hat{\mathbf{z}} \times (1/f)\mathbf{r}\phi(0)$ is the surface geostrophic current. However, (57) implies that P also must be subtracted before this is a correct interpretation. This final correction is not currently being made, as far as we know.

4. Empirical estimates of the wave effects

An assessment of the wave-generated effects in the large-scale circulation model presented in the previous section could be made by evaluating the relevant quantities from a wave climatology. However, since surface wind climatologies are both more complete and more readily available, we instead base our empirical estimates on a wind climatology from a reanalysis using an operational weather forecast model for the years 1979–95 (Kalnay et al. 1996). In the estimates that follow we assume that the waves are fully developed and in local equilibrium with the local wind on circulation timescales. Obviously, this is not entirely correct. In particular, the following estimates do not include remotely generated swell, which often is a substantial component of the wave field. Nevertheless, this initial assessment illustrates the nature of the wave effects on the circulation. It may later be possible to obtain improved estimates from a wave-dynamical model used in an operational forecasting mode, such as the one by the

WAMDI Group (1988) currently in use at the European Centre for Medium-Range Weather Forecasts.

To make the estimates, we rely on the empirically fitted wave spectrum of Pierson and Moskowitz (1964). We shall assume that the wave dynamics are linear and conservative to leading order, as in section 2, to derive wave–wind relations in a way that closely parallels Kenyon (1969). As in Phillips (1977, chapter 4), we define the directional horizontal wavenumber spectrum, $\mathcal{P}(k, \alpha)$, for the surface waves as

$$\begin{aligned} \langle(\eta^w)^2\rangle &= \int_{-\infty}^{+\infty} \int_{-\infty}^{+\infty} F(\mathbf{k}_h) d\mathbf{k}_h \\ &= \int_0^\infty \int_0^{2\pi} \mathcal{P}(k, \alpha) k dk d\alpha, \end{aligned} \tag{58}$$

where (k, α) is a cylindrical coordinate representation of \mathbf{k}_h . We assume local isotropy in the wave spectra on large spatial scales, so that

$$k\mathcal{P}(k, \alpha) = \left| \frac{d\sigma}{dk} \right| f(\sigma)S(\alpha), \tag{59}$$

where

$$\int_0^{2\pi} S(\alpha) d\alpha = 1,$$

and $\sigma = \sqrt{gk}$. Thus,

$$\langle(\eta^w)^2\rangle = \int_0^\infty f(\sigma) d\sigma. \tag{60}$$

Likewise, referring to (25),

$$P = \langle(\eta^w)^2\rangle = \int_0^\infty \sigma^2 f(\sigma) d\sigma, \tag{61}$$

and the Stokes drift velocity, as previously derived by Kenyon [1969, Eq. (8)], is

$$\mathbf{u}^s = \hat{\mathbf{e}}_h \frac{2}{g} \int_0^\infty f(\sigma)\sigma^3 \exp\left[\frac{2\sigma^2 z}{g}\right] d\sigma, \tag{62}$$

where $\hat{\mathbf{e}}_h$ is the dominant direction of wave propagation, which is assumed to coincide with the wind direction.

Pierson and Moskowitz (1964) fitted empirical spectra of the following form for the ocean wave field under fully developed conditions in deep water:

$$f_n(\sigma) = \frac{a_n g^2}{\sigma^5} \exp\left[-b_n \left(\frac{g}{W\sigma}\right)^n\right], \tag{63}$$

where $n = 2, 3, 4$ are alternative fits, $W = |\mathbf{U}_a|$ is the wind speed, and the associated constants are

$$\begin{aligned} a_n &= \left(\frac{f_o}{2\pi}\right)(2\pi\nu_o)^5 e^{5/n}, & b_n &= \left(\frac{5}{n}\right)(2\pi\nu_o)^n, \\ f_o &= 0.0275, & \nu_o &= 0.140. \end{aligned} \tag{64}$$

After inserting (63) into (60) and (61), we obtain the closed-form expressions

$$\begin{aligned} \langle(\eta^w)^2\rangle &= \frac{a_n W^4}{ng^2 b_n^{4/n}} \Gamma\left[1 + \frac{5}{n}\right] \\ P &= \frac{a_n W^2}{nb_n^{2/n}} \Gamma\left[1 + \frac{3}{n}\right], \end{aligned} \tag{65}$$

by making use of the definition of the Gamma function, $\Gamma[\gamma] = \int_0^\infty s^{\gamma-1} e^{-s} ds$. Kenyon [1969, Eq. (13)] gives a closed-form expression for the drift velocity using the Pierson–Moskowitz spectra when $n = 2$. Accordingly, we restrict our estimates to the $n = 2$ fit, whence the final formulas for the wave quantities in our wind-fitted model are

$$\begin{aligned} \langle(\eta^w)^2\rangle &= (1.3 \times 10^{-4} s^4 m^{-2}) W^4 \\ \frac{1}{g} P &= (1.0 \times 10^{-3} s^2 m^{-1}) W^2 \\ \mathbf{u}^s(z) &= 0.04 \mathbf{U}_a \exp\left[-\frac{4\sqrt{g|z|}}{W}\right]. \end{aligned} \tag{66}$$

Furthermore, we can readily integrate the Stokes-drift profile in the vertical to obtain a Stokes transport formula,

$$\mathbf{T}_{st} = (5.1 \times 10^{-4} s^2 m^{-1}) W^2 \mathbf{U}_a, \tag{67}$$

which is equal to \mathbf{M} from (23) for periodic linear waves.

An empirically established bulk formula for wind stress is

$$\boldsymbol{\tau} = \rho_a C_D W \mathbf{U}_a, \tag{68}$$

where ρ_a is the atmospheric surface density and C_D is the drag coefficient. We use the formulation of Large and Pond (1982) for C_D , and then calculate $\boldsymbol{\tau}$ by (68) by the procedure described in Trenberth et al. (1989).

Using the preceding relations for the Stokes transport and wind stress, we can derive an alternative formula for \mathcal{R} , defined in (54), which exposes its dependencies on the most geographically variable quantities (viz., f and \mathbf{U}_a), ignoring its other dependencies. The result is

$$\mathcal{R} \propto \frac{1}{|f\mathbf{U}_a|}. \tag{69}$$

Thus, we see that a high wind regime favors the wave-driving influence, while weak winds favor the wind driving unless the local waves are enhanced through remotely generated swell. Moreover, the wave-driving influence tends to increase with latitude since $|f|$ does, and from (56), we can attribute this to the decrease in the Ekman-layer depth. Since wind speeds also tend to be larger in middle and high latitudes, at least in winter, both factors in (69) indicate that the wave driving is relatively more important in these regions.

Equations (66)–(68) are fully determined from $\mathbf{U}_a(\mathbf{x}_h, t)$, which we obtain from the 17-yr wind cli-

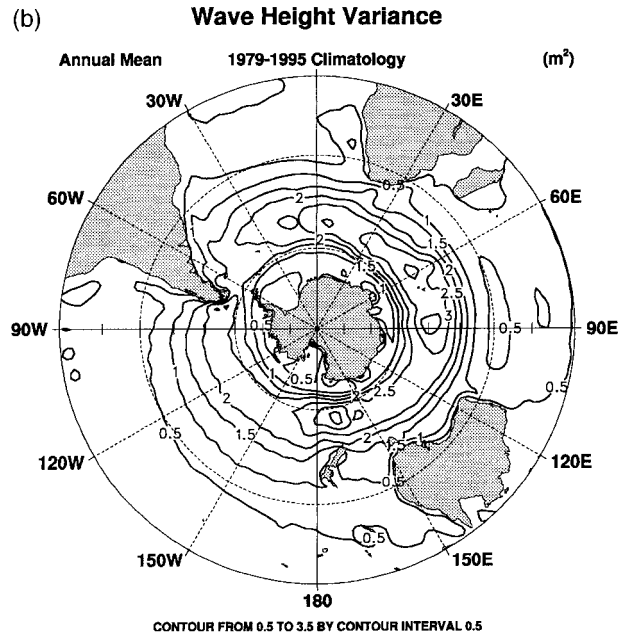
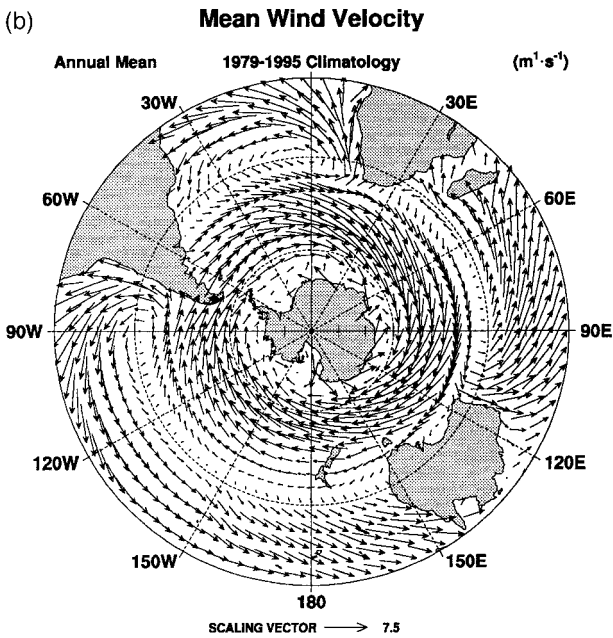
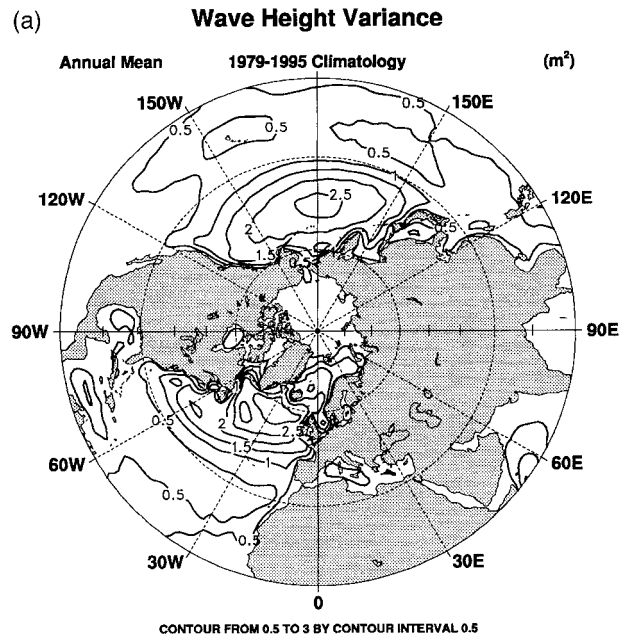
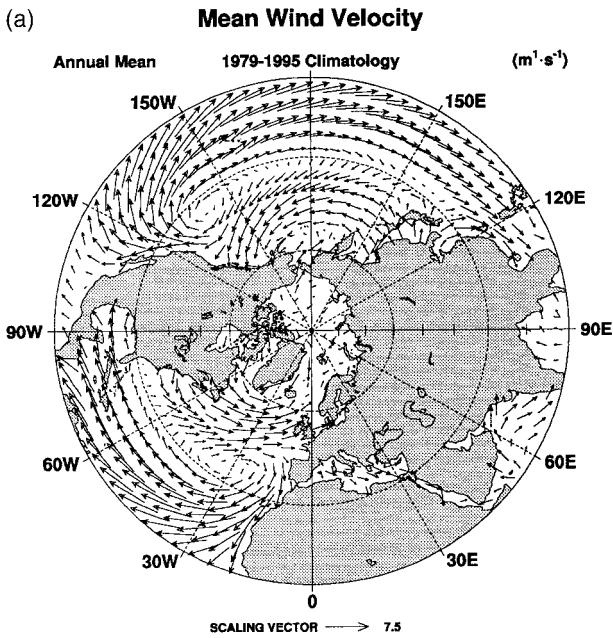


FIG. 1. Annual-mean wind, U_a , at a height of 10 m above the sea surface: (a) Northern Hemisphere; (b) Southern Hemisphere.

FIG. 2. Annual-mean wave height variance, $\langle(\eta^w)^2\rangle$, from (66): (a) Northern Hemisphere; (b) Southern Hemisphere.

matology of Kalnay et al. (1996). This climatology contains a wind field every 6 h on a T62 spatial grid (i.e., with a lat-long resolution finer than 2°). In this paper we show only the time-mean fields, in a polar stereographic format separately for each hemisphere.

The near-surface wind pattern in this climatology (Fig. 1) shows the expected features: zonally oriented tropical trade winds, midlatitude westerlies, and weak polar easterlies; the Afro-Asian monsoon; and the

standing-eddy circulations of subtropical anticyclones and subpolar cyclones.

The mean strength of the waves, $\langle(\eta^w)^2\rangle$ from (66), is shown in Fig. 2. The waves are strongest in the midst of the westerly winds, away from land, and the variance ranges from less than 0.5 m^2 in the Tropics to more than 3 m^2 in both hemispheres.

The mean wave-averaged correction to the surface pressure boundary condition (25), that is $P = \langle(\eta^w)^2\rangle$ from (66), is shown in Fig. 3, with a further division

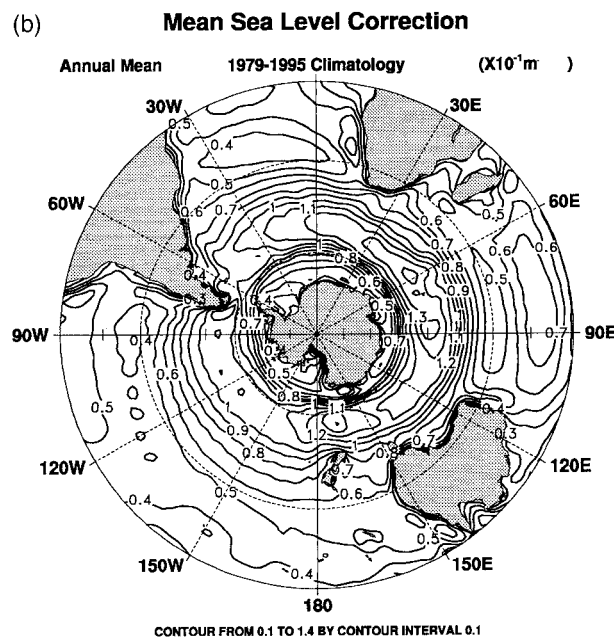
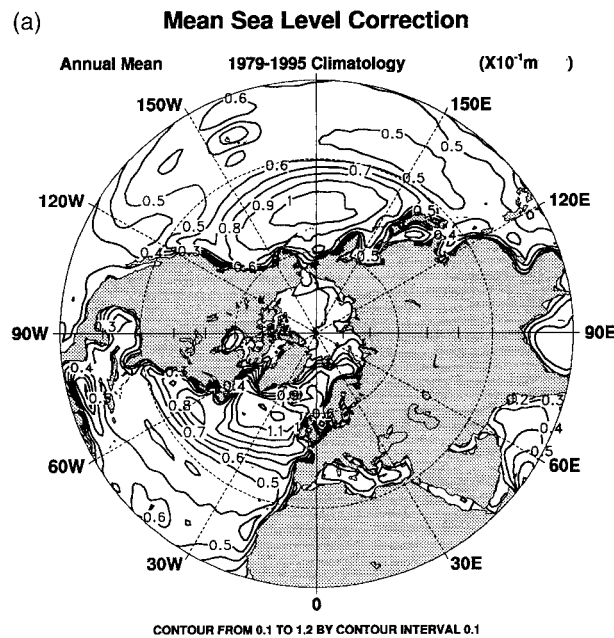


FIG. 3. Annual-mean increment to the surface-pressure boundary condition, that is, $g^{-1}P$ from (66): (a) Northern Hemisphere; (b) Southern Hemisphere.

by g so that it can be interpreted as an equivalent sea level correction. The spatial pattern is qualitatively similar to that in Fig. 2, ranging from about 0.04 m in the Tropics to above 0.12 m (Northern Hemisphere) or 0.14 m (southern) in the subpolar regions. This quantity weakens near Antarctica and in the Arctic Ocean, where in addition sea ice frequently suppresses the surface waves altogether.

The Stokes transport, \mathbf{T}_{st} from (67), is shown in Fig.

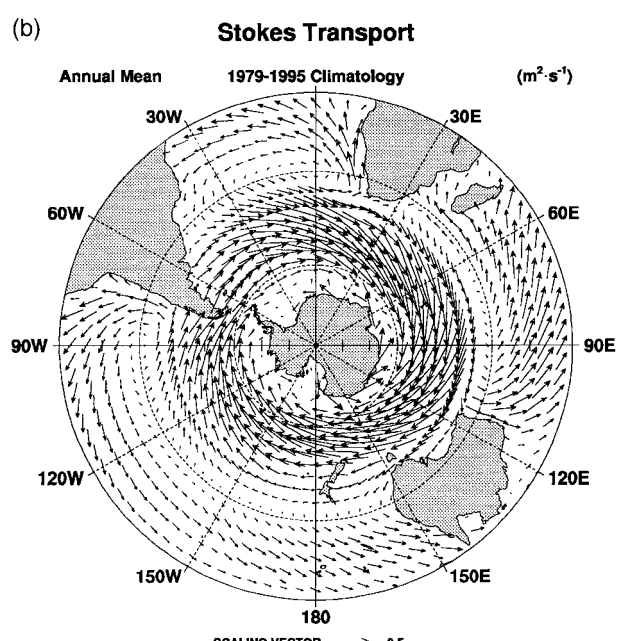
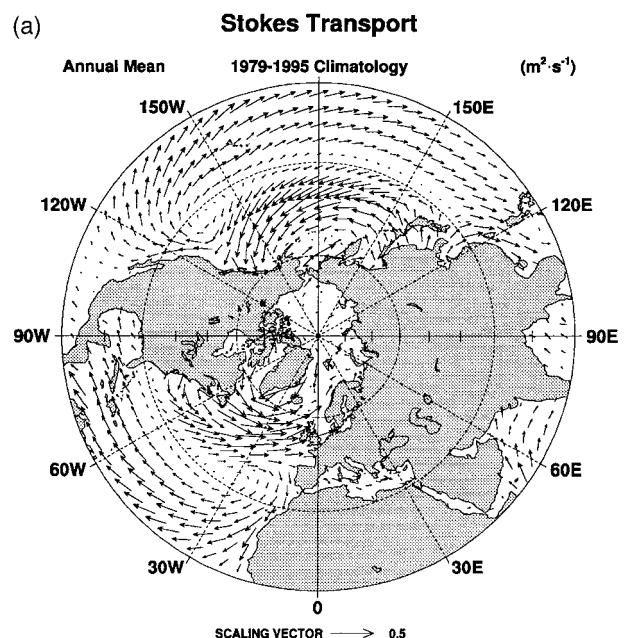


FIG. 4. Annual-mean Stokes transport, \mathbf{T}_{st} from (67): (a) Northern Hemisphere; (b) Southern Hemisphere.

4. The nonlinear dependence on the near-surface wind enhances the spatial contrast in amplitude here, but the directions are similar to those in Fig. 1. The westerly wind regimes between about 40° and 60° have the strongest Stokes transports, with a magnitude approaching $1 \text{ m}^2 \text{ s}^{-1}$.

For comparison, the Lagrangian Ekman transport, $-\hat{\mathbf{z}} \times (1/f\rho_0)\boldsymbol{\tau}^t$ from (51) and (68), is shown in Fig. 5. Its pattern differs from that of \mathbf{T}_{st} both in its larger tropical and subtropical magnitudes and its approximate or-

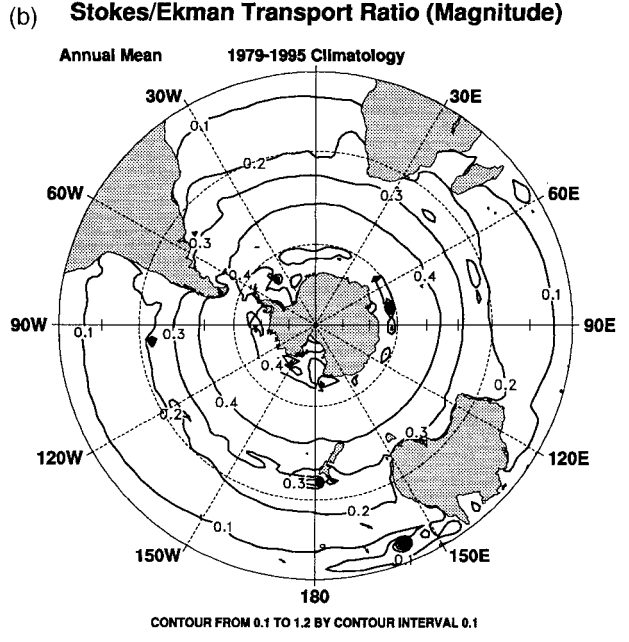
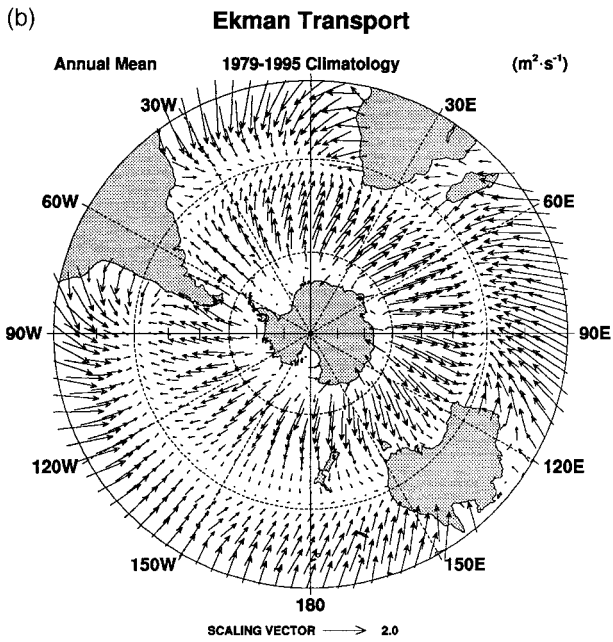
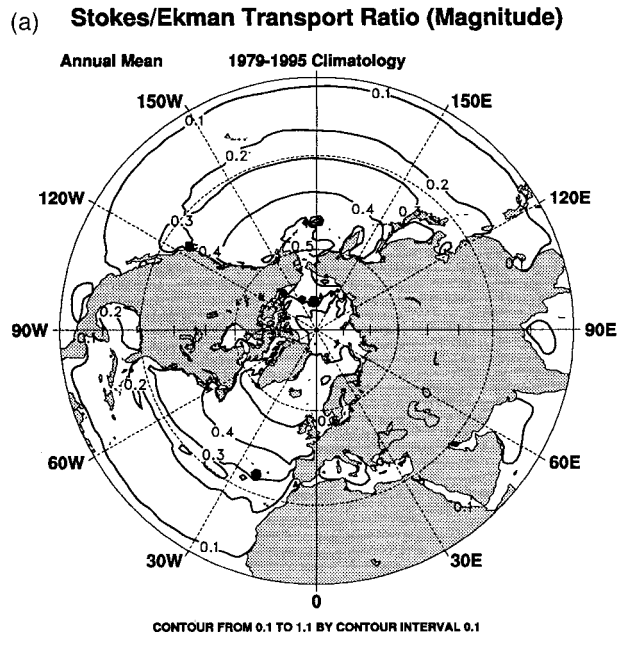
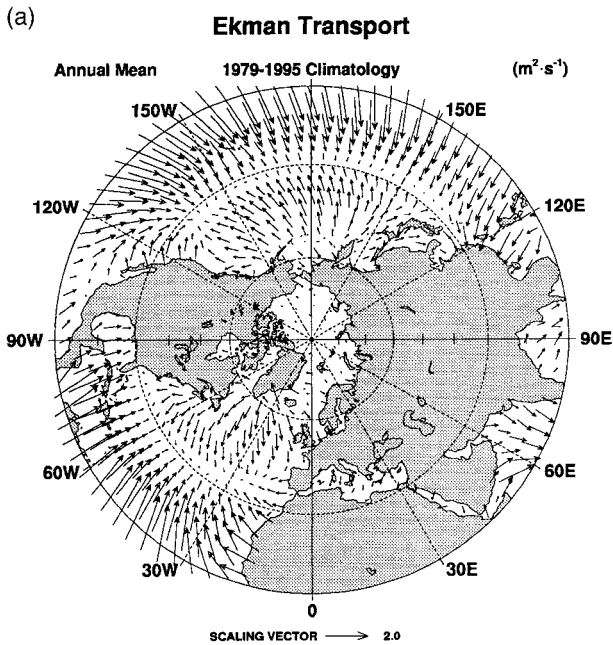


FIG. 5. Annual-mean Lagrangian Ekman transport $-\hat{z} \times (1/f\rho_0)\tau'$ from (68): (a) Northern Hemisphere; (b) Southern Hemisphere.

FIG. 6. The ratio of the wave- and wind-driven components in (51), $1/\mathcal{R}$ from (54), using the fields in Figs. 4–5. The contour interval is 0.1. The largest contour of 1.0 is approached only where $|\mathbf{U}_d| \rightarrow 0$.

thogonality in direction (which, again, indicates that this aspect is not changed by the nonlinearity of the wind dependences). The magnitude of the Lagrangian Ekman transport is much larger than \mathbf{T}_{st} near the equator, but these two quantities have opposite trends with increasing latitude. The Stokes transport fraction grows to a level of more than 40% of the Lagrangian Ekman transport at higher latitudes. This confirms the estimate in (69).

Previous empirical tests of Ekman and Sverdrup

transport relations have largely been confined to relatively low latitudes. From Fig. 6, it is clear that this is a region where they are best satisfied and the wave effects are smallest. For example, Chereskin (1995) found an empirical agreement in the California Current between the Ekman transport relation to the surface wind stress, with a relative uncertainty of about 20%. This analysis is for the summer half of the year and neglects wave effects. This conclusion is marginally

consistent with the annual-mean \mathcal{R} value there (Fig. 6), and it is even more consistent with the smaller \mathcal{R} value that occurs during the summer season (not shown). There would be a larger signal-to-noise ratio for testing the Stokes transport contribution at higher latitudes and during the winter season.

5. Summary and discussion

In the present study we have followed the approach of Craik and Leibovich (1976) to derive a generalized Boussinesq model for oceanic currents in which the average dynamical effects of the gravity wave field are taken into account. The prescription is very general: it relies on the decomposition of the dynamics in terms of rapidly and slowly varying components, where the former is approximately an irrotational flow with zero Eulerian time average but nonzero Lagrangian average. The surface waves contribute to the slow-time dynamics via the Stokes drift and wave-averaged modifications to the boundary conditions.

In a first step toward the oceanic context, we assume that the irrotational wave field is composed of nondissipative, deep-water waves with small wave slope and use this solution form to derive the Stokes drift and leading-order approximations for other wave-averaged contributions. We use an empirical specification of the wave spectrum in lieu of theoretically addressing the nonlinear, nonconservative higher-order wave dynamics. In this formulation, the important wave-added terms in the model are the following: Stokes-drift vortex and Coriolis forces, a Stokes-drift tracer advection, a Stokes-drift transport divergence in the surface kinematic boundary condition for vertical velocity, and a sea level tendency variance increment to the surface pressure boundary condition.

In a second step toward a particular oceanic dynamical regime, further approximations are made appropriate to a wave field with large-scale, slow-time variations in its spectrum and large-scale, wave-averaged currents away from regions of narrow intense flow (e.g., near the western boundary). This leads to the generalized planetary geostrophic equations that retain several of the wave-added terms. Analyses are made for solution properties that are independent of particular parameterizations for smaller-scale tracer and momentum fluxes, such as the surface boundary-layer transport, the interior geostrophic momentum and planetary vorticity balances, and the depth-integrated transport. We show that the traditional relations for the Ekman and Sverdrup transports as functionals of the surface wind stress apply to the total Lagrangian-mean transport, not the Eulerian-mean as usually stated, where the Stokes transport is a component of the Lagrangian mean. This implies that these Eulerian-mean transports have a Stokes-canceling component, albeit with a different depth profile than the Stokes-drift velocity. The wave-added contribution to the surface pressure boundary condition modifies the

usual inverse-barometer and surface geostrophic dynamic height relations; an implication of this is that the inferences of surface geostrophic dynamic height from atmospheric surface pressure and altimetric sea level measurements should include the wave effect.

Under the assumption that both the surface stress and surface gravity wave spectrum are in equilibrium with the surface wind, we use empirical regression formulas to estimate some of the important wave-added fields from a global wind climatology. These estimates show that the wave effects are more significant at higher latitudes where the winds are stronger. In particular, in the midlatitude westerly wind regime, the Stokes transport is a significant fraction of the Ekman transport and the wave-tendency variance is a significant fraction of the mean surface geostrophic dynamic height. In subtropical and equatorial regions, in contrast, the wave-added effects are usually small compared to the wind stress effects. The present empirical analysis is only a preliminary one in several respects. Obvious future extensions are to the low-frequency, basin-scale variability; the remotely generated swell component; and estimates directly from either wave observations or wave-forecast models that can also include disequilibrium wave processes. These extensions would permit the very interesting process of remote generation of currents by propagating, evolving wave fields.

The wave-averaged theory makes predictions that need observational or laboratory testing. This is probably not easy to do comprehensively. Even the Stokes drift itself has only been measured poorly and incompletely in the ocean, and it may be more prudent to rely on at least this (ancient) part of the theory than to attempt its direct measurement. The two types of tests that seem to us most interesting and feasible are for the Eulerian Ekman transport (51)—or its pointwise velocity counterpart—and for the relationship between the wave-averaged sea level and surface geostrophic current [i.e., the gradient of the first condition in (37)]. Both of these tests can be made over a small geographical region, over a short time interval of days, and with only near-surface measurements. Obviously, it would be sensible to make these tests of the wave effects where the signal-to-noise ratios are favorable, which occurs in high wave conditions, as in extratropical latitudes in the winter season. We do not suggest specific experimental designs here.

An oceanic general circulation model (OGCM) could easily be generalized to incorporate the wave-added dynamical effects derived here. The relevant fluid-dynamical model is the hydrostatic primitive equations with tracer equations for potential temperature and salinity and the true equation of state for seawater. All of the extra terms in section 2 should be included, except in the surface stress condition (27) [for the reason explained in the discussion following (33)]. Furthermore, if a more general free-surface condition were preferred [e.g., as discussed following (23)], it could be used in-

stead of the rigid-lid approximation presented here. Including these wave-added effects in an OGCM requires either a companion large-scale wave model or a climatological dataset for the wave properties (as in section 4). Even though our empirical estimates indicate that some of the wave-added effects are significant in middle- and high-latitude regions, we can anticipate that certain aspects of an OGCM solution will change relatively little, due to several partial cancellations in the wave-modified solutions. An example of this is the cancellation between horizontal boundary-layer transport convergence and the surface vertical velocity in the resulting Ekman pumping at the base of the boundary layer, which leaves the interior geostrophic circulation unaffected by waves [see (53)]. Another example is the partial cancellation (i.e., in the integral over depth) between the horizontal currents advecting the tracer fields and the wave-added Stokes-drift advection of the Eulerian current, which tends to have a Stokes-compensating component [e.g., as in (51)]; this leaves only the difference in their vertical profiles as the noncancelling part of the advecting velocity.

In summary, we believe that this wave-averaged theory is relevant to many oceanic current regimes, and that at least some of its predictions can feasibly be tested by observations. Its consequences are likely to be significant for the large-scale, wind-driven circulation. These remarks pertain both to the particular simple wind-gyre solutions presented here, as well to more general ones for which the wave-averaged Boussinesq model is relevant.

Acknowledgments. We appreciate comments from Russ Davis, Darryl Holm, William Large, Sidney Leibovich, Jerry Smith, Remi Tailleux, and Greg Eyink. We are especially grateful to Doug Lindholm and Kevin Trenberth for performing the climatological calculations presented in section 4 (with support from NOAA/NASA Grant NA56GP0576). This research was supported by the Office of Naval Research (ONR-N00014-92-F-0117; ONR-N00014-95-1-0316) and the National Science Foundation (OCE-9633681).

APPENDIX A

Wave Transport in the Vorticity Equation

Here we calculate

$$\nabla \times \langle \mathbf{u}^w \times \boldsymbol{\omega}_1 \rangle = \langle \boldsymbol{\omega}_1 \cdot \nabla \mathbf{u}^w \rangle - \langle \mathbf{u}^w \cdot \nabla \boldsymbol{\omega}_1 \rangle \quad (\text{A1})$$

in Eq. (15), with

$$\boldsymbol{\omega}_1 = \nabla \times (\mathbf{U} \times \mathbf{Z}),$$

where $\mathbf{U} \equiv \int^t \mathbf{u}^w(\cdot, s) ds$ and $\mathbf{Z} \equiv \boldsymbol{\omega}_0 + 2\boldsymbol{\Omega}$. The following derivation follows the methodology established in CL. It corrects a minor typographical error in the original Craik and Leibovich (1976) calculation [cf. Eq. (11) in their paper] and differs from the original by the inclusion of Coriolis forces.

We begin by stating some relations that will be useful in the calculation. Since \mathbf{u}^w has zero divergence, so too does \mathbf{U} . By definition $\boldsymbol{\omega}_0$ has zero divergence and it is easily verified that $\nabla \cdot \boldsymbol{\omega}_1 = 0$ here. The averages are such that $\langle \mathbf{Z} \rangle = \mathbf{Z}$, since $\langle \boldsymbol{\omega}_0 \rangle = \boldsymbol{\omega}_0$ and $\langle 2\boldsymbol{\Omega} \rangle = 2\boldsymbol{\Omega}$.

Next, we show that the Stokes drift has no divergence,

$$\nabla \cdot \mathbf{u}^s = 0.$$

Using tensor notation with a comma denoting differentiation, the k th component of the Stokes-drift velocity is the time average of $U_j u_{kj}^w$. The quantity

$$\frac{\partial}{\partial t} [(U_j U_{j,k})_{,k}] = u_{j,k}^w U_{k,j} + U_{j,k} u_{k,j}^w$$

is an identity since the velocity is divergence free. Furthermore, since the velocity is periodic and the time average $\langle \mathbf{u}^w \rangle$ is zero, the left-hand side of the above expression is identically zero and thus Stokes drift is solenoidal.

Now we proceed to calculate (A1). The following vector identity is used frequently:

$$\begin{aligned} \text{curl}(\mathbf{A} \times \mathbf{B}) &= \mathbf{A} \text{div} \mathbf{B} - \mathbf{B} \text{div} \mathbf{A} + (\mathbf{B} \cdot \text{grad}) \mathbf{A} \\ &\quad - (\mathbf{A} \cdot \text{grad}) \mathbf{B}, \end{aligned}$$

for arbitrary vectors \mathbf{A} and \mathbf{B} . Substituting (14) into (A1) yields

$$\begin{aligned} \{ \nabla \times \langle \mathbf{u}^w \times \boldsymbol{\omega}_1 \rangle \}_i &= \langle Z_k U_{j,k} u_{i,j}^w \rangle - \langle U_j Z_{k,j} u_{i,k}^w \rangle + \langle u_k^w (U_j Z_{i,j})_{,k} \rangle \\ &\quad - \langle u_k^w (Z_j U_{i,j})_{,k} \rangle + \langle Z_{k,k} U_j u_{i,j}^w \rangle \\ &\quad - \langle \{ \mathbf{u}^w \cdot \nabla [\mathbf{U} \nabla \cdot \mathbf{Z}] \} \}_i. \end{aligned} \quad (\text{A2})$$

The implications of a nonsolenoidal $\boldsymbol{\Omega}$ will be considered briefly in appendix B. Here, however, we consider the geophysical setting, in which $\boldsymbol{\Omega}$ is spatially uniform in an inertial frame, hence $\nabla \cdot 2\boldsymbol{\Omega} = 0$ in a geocentric rotating frame. Thus, the last two terms in (A2) vanish.

The first term in (A2) can be shown to be

$$\langle Z_k U_{j,k} u_{i,j}^w \rangle = Z_k u_{i,k}^s - Z_k \langle U_j u_{i,jk}^w \rangle, \quad (\text{A3})$$

where $u_i^s \equiv \langle U_j u_{ij}^w \rangle$ is the Stokes-drift velocity. Since

$$\left\langle \frac{\partial}{\partial t} (U_j U_k) \right\rangle = \langle u_j^w U_k + U_j u_k^w \rangle$$

and the left-hand side of this expression is identically zero, we can write the third term in (A2) as

$$\langle u_k^w (U_j Z_{i,j})_{,k} \rangle = \langle u_k^w Z_{i,jk} U_j \rangle - \langle U_k Z_{i,j} u_{j,k}^w \rangle.$$

However, the first term on the right-hand side of this expression is zero, since $Z_{i,jk}$ is symmetric and $u_k^w U_j$ is antisymmetric. The second term, on the other hand, can be identified as $-Z_{i,j} u_j^s$. It is easy to see that the second term of (A3) cancels with the second and fourth terms of (A2). Hence, Eq. (A2) may be written as

$$\{\nabla \times \langle \mathbf{u}^w \times \boldsymbol{\omega}_1 \rangle\}_i = Z_k u_{i,k}^s - Z_{i,k} u_i^s = \{\nabla \times (\mathbf{u}^s \times \mathbf{Z})\}_i, \quad (\text{A4})$$

APPENDIX B

Vortex Force with a Nonsolenoidal Rotation Vector

In this appendix we briefly consider the implications of a nonzero $\nabla \cdot 2\boldsymbol{\Omega}$ on the vortex force.

Taking into account the results of appendix A and assuming that $2\boldsymbol{\Omega}$ is not divergence free, the vortex force may be written as

$$\{\nabla \times \langle \mathbf{u}^w \times \boldsymbol{\omega}_1 \rangle\}_i = Z_k u_{i,k}^s - Z_{i,k} u_i^s + Z_{k,k} u_i^s - \langle \{\mathbf{u}^w \cdot \nabla[\mathbf{U}\nabla \cdot \mathbf{Z}]\}_i \rangle, \quad (\text{B1})$$

where the fifth term (A2) was replaced by its equivalent $Z_{k,k} u_i^s$. Since the divergence of the first three terms on the right-hand side is identically zero, we can write it as a curl of a quantity. This implies that the divergence of the last term must also be zero, which is verified below. Thus,

$$\{\nabla \times \langle \mathbf{u}^w \times \boldsymbol{\omega}_1 \rangle\}_i = \langle \{\nabla \times (\mathbf{u}^w \times \mathbf{Z})\}_i \rangle - \langle \{\mathbf{u}^w \cdot \nabla[\mathbf{U}\nabla \cdot \mathbf{Z}]\}_i \rangle. \quad (\text{B2})$$

Now we consider the last term in the above equation. First note that $\nabla \cdot \mathbf{Z} = \nabla \cdot 2\boldsymbol{\Omega}$. Next we verify that the last quantity in (B2) is divergence free:

$$[u_j^w \langle \zeta U_i \rangle_{,j}]_i = \zeta U_{i,j} u_{j,i}^w + \zeta_{,j} U_i u_{j,i}^w + \zeta_{,i} u_j^w U_{i,j} + \zeta_{,ij} U_j u_i^w = 0, \quad (\text{B3})$$

with $\zeta \equiv \nabla \cdot 2\boldsymbol{\Omega}$, hence it is expressible in terms of the curl of another quantity.

Let $W_{ij} \equiv \langle U_i u_j^w \rangle$. This quantity has the property that $W_{ij,i} = u_j^s$ and $W_{ij,j} = -u_i^s$ and hence is antisymmetric, thus implying that $W_{ij} = \epsilon_{ijk} \chi_k^s$, where ϵ_{ijk} is the cyclic operator and $\boldsymbol{\chi}^s$ is a vector streamfunction for the Stokes drift velocity. That is,

$$u_i^s = -W_{ij,j} = -\epsilon_{ijk} \chi_{k,j}^s = -(\nabla \times \boldsymbol{\chi}^s)_i.$$

Taking the curl of this expression yields,

$$\Delta \boldsymbol{\chi}^s = \boldsymbol{\omega}^s,$$

assuming $\nabla \cdot \boldsymbol{\chi}^s = 0$, where $\boldsymbol{\omega}^s$ is the vorticity of the Stokes-drift velocity.

We can write the explicit expression for the second term on the right-hand side of (B2) as the curl of some quantity,

$$\langle \{(u_j^w U_i \zeta)_{,j}\}_i \rangle = \nabla \times (\zeta \boldsymbol{\chi}^s),$$

since

$$\begin{aligned} \langle (u_j^w U_i \zeta)_{,j} \rangle &= -u_i^s \zeta + W_{ij} \zeta_{,j} = -u_i^s \zeta + \epsilon_{ijk} \chi_k^s \zeta_{,j} \\ &= -u_i^s \zeta + \{\nabla \zeta \times \boldsymbol{\chi}^s\}_i \\ &= \{\nabla \times \boldsymbol{\chi}^s\}_i \zeta + \{\nabla \zeta \times \boldsymbol{\chi}^s\}_i. \end{aligned} \quad (\text{B4})$$

To summarize,

$$\begin{aligned} \nabla \times \langle \mathbf{u}^w \times \boldsymbol{\omega}_1 \rangle &= \nabla \times (\mathbf{u}^s \times \mathbf{Z}) - \nabla \times [(\nabla \cdot \mathbf{Z}) \boldsymbol{\chi}^s] \\ &= (\boldsymbol{\omega}_0 + 2\boldsymbol{\Omega}) \cdot \nabla \mathbf{u}^s - \mathbf{u}^s \cdot \nabla (\boldsymbol{\omega}_0 + 2\boldsymbol{\Omega}) \\ &\quad + (\nabla \cdot 2\boldsymbol{\Omega}) \mathbf{u}^s - \nabla \times [(\nabla \cdot 2\boldsymbol{\Omega}) \boldsymbol{\chi}^s]. \end{aligned} \quad (\text{B5})$$

APPENDIX C

Wave Transport in the Tracer Equation

Here we provide the details of the calculation of

$$\langle \mathbf{u}^w \cdot \nabla \theta_1 \rangle$$

after (30) is replaced in Eq. (31). With the help of an identity,

$$\begin{aligned} \langle \{\mathbf{u}^w \cdot \nabla(\mathbf{U} \cdot \nabla \theta)\}_i \rangle &= \langle \{\nabla \cdot (\mathbf{u}^w \nabla \cdot (\theta \mathbf{U}))\}_i \rangle \\ &= \langle u_i^w (U_j \theta_{,j})_{,i} \rangle. \end{aligned}$$

However,

$$\langle u_i^w (U_j \theta_{,j})_{,i} \rangle = \langle u_i^w U_{j,i} \theta_{,j} \rangle + \langle u_i^w U_j \theta_{,ji} \rangle. \quad (\text{C1})$$

The first term on the right-hand side of the above equation can be shown to satisfy

$$\langle u_i^w U_{j,i} \theta_{,j} \rangle = \left\langle \frac{\partial}{\partial t} (U_i U_j) \theta_{,ji} \right\rangle - \langle U_i u_{j,i}^w \theta_{,j} \rangle,$$

and with time averaging the time derivative term is zero. Thus,

$$\langle u_i^w U_{j,i} \theta_{,j} \rangle = -u_i^s \langle \theta_{,j} \rangle.$$

Again, since the time average of a time derivative must vanish, the following equation shows that the second term in (C1) vanishes:

$$\frac{\partial}{\partial t} (U_i U_j) \theta_{,ji} = u_i^w U_j \theta_{,ji} + u_i^w U_j \theta_{,ji} = 2u_i^w U_j \theta_{,ji}.$$

At this stage, all the terms can be replaced in (31), and then a time average is performed. With $\mathbf{u}_j^s = \langle U_i u_{j,i}^w \rangle$, the time-averaged tracer equation is then (32).

REFERENCES

- Andrews, D. G., and M. E. McIntyre, 1978: An exact theory of nonlinear waves on a Lagrangian-mean flow. *J. Fluid Mech.*, **89**, 609–646.
- Chereskin, T. K., 1995: Direct evidence for an Ekman balance in the California Current. *J. Geophys. Res.*, **100**, 18 261–18 269.
- Craik, A. D. D., 1982: The generalized Lagrangian-mean equations and hydrodynamic stability. *J. Fluid Mech.*, **125**, 27–35.
- , and S. Leibovich, 1976: A rational model for Langmuir circulations. *J. Fluid Mech.*, **73**, 401–426.
- Ekman, V. W., 1905: On the influence of the Earth's rotation on ocean currents. *Matem. Astr. Fysik.*, **2**(11).
- Gnanadesikan, A., and R. A. Weller, 1995: Structure and instability of the Ekman spiral in the presence of surface gravity waves. *J. Phys. Oceanogr.*, **25**, 3148–3171.
- Hasselmann, K., 1970: Wave-driven inertial oscillations. *Geophys. Fluid Dyn.*, **1**, 463–502.
- , 1971: On the mass and momentum transfer between short grav-

- ity waves and larger-scale motions. *J. Fluid Mech.*, **50**, 189–205.
- Hautala, S. L., D. H. Roemmich, and W. J. Schmitz, 1994: Is the North Pacific in Sverdrup balance along 24° N? *J. Geophys. Res.*, **99**, 16 041–16 052.
- Holm, D. D., 1996: The ideal Craik–Leibovich equations. *Physica D*, **98**, 415–441.
- Huang, N. E., 1979: On surface drift currents in the ocean. *J. Fluid Mech.*, **91**, 191–208.
- Kalnay, E., and Coauthors, 1996: The NCEP–NCAR 40-Year Reanalysis Project. *Bull. Amer. Meteor. Soc.*, **77**, 437–471.
- Kenyon, K. E., 1969: Stokes drift for random gravity waves. *J. Geophys. Res.*, **74**, 6991–6994.
- Large, W. G., and S. Pond, 1982: Sensible and latent heat flux measurements over the ocean. *J. Phys. Oceanogr.*, **12**, 464–484.
- Leetmaa, A., P. P. Niiler, and H. Stommel, 1977: Does the Sverdrup relation account for the Mid-Atlantic Circulation? *J. Marine Res.*, **36**, 311–322.
- Leibovich, S., 1977a: On the evolution of the system of wind drift currents and Langmuir circulations in the ocean. Part I: Theory and averaged current. *J. Fluid Mech.*, **79**, 715–743.
- , 1977b: Convective instability of stably stratified water in the ocean. *J. Fluid Mech.*, **82**, 561–581.
- , 1980: On wave–current interaction theories of Langmuir circulations. *J. Fluid Mech.*, **99**, 715–724.
- , 1983: The form and dynamics of Langmuir circulations. *Annu. Rev. Fluid Mech.*, **15**, 391–427.
- Longuet-Higgins, M. S., 1953: Mass transport in water waves. *Philos. Trans. Roy. Soc. London*, **245**, 535–581.
- , and R. W. Stewart, 1960: Changes in the form of short gravity waves on long waves and tidal currents. *J. Fluid Mech.*, **8**, 565–583.
- , and ———, 1961: The changes in amplitude of short gravity waves on steady non-uniform currents. *J. Fluid Mech.*, **10**, 529–549.
- McWilliams, J. C., 1996: Modeling the oceanic general circulation. *Annu. Rev. Fluid Mech.*, **28**, 1–34.
- , P. P. Sullivan, and C.-H. Moeng, 1997: Langmuir turbulence in the ocean. *J. Fluid Mech.*, **334**, 1–30.
- Munk, W. H., 1950: On the wind-driven ocean circulation. *J. Meteor.*, **7**, 79–93.
- Pedlosky, J., 1996: *Ocean Circulation Theory*. Springer-Verlag, 453 pp.
- Phillips, O. M., 1977: *The Dynamics of the Upper Ocean*. Cambridge University Press, 336 pp.
- Pierson, W. J., and L. Moskowitz, 1964: A proposed spectral form for fully developed wind seas based on the similarity theory of S. A. Kitaigorodskii. *J. Geophys. Res.*, **69**, 5181–5190.
- Roemmich, D., and C. Wunsch, 1985: Two transatlantic sections: Meridional circulation and heat flow in the subtropical North Atlantic Ocean. *Deep-Sea Res.*, **32**, 619–664.
- Smith, J., 1992: Observed growth of Langmuir circulation. *J. Geophys. Res.*, **97**, 5651–5664.
- Stokes, G. G., 1847: On the theory of oscillatory waves. *Trans. Cambridge Philos. Soc.*, **8**, 441–455.
- Stommel, H., 1948: The westward intensification of wind-driven ocean currents. *Trans. Amer. Geophys. Union*, **29**, 202–206.
- Sverdrup, H. U., 1947: Wind-driven currents in a baroclinic ocean: With application to the equatorial currents of the eastern Pacific. *Proc. Natl. Acad. Sci.*, **33**, 318–326.
- Trenberth, K. E., J. G. Olson, and W. G. Large, 1989: A global ocean wind stress climatology based on ECMWF analyses. NCAR Tech. Note. NCAR/TN-338 + STR, NCAR, 93 pp. [Available from NCAR, P.O. Box 3000, Boulder, CO 80307.]
- WAMDI Group, 1988: The WAM model—A third-generation ocean wave prediction model. *J. Phys. Oceanogr.*, **18**, 1775–1810.
- Webber, J. E., 1983: Steady wind- and wave-induced currents in the upper ocean. *J. Phys. Oceanogr.*, **13**, 524–530.
- , and A. Melsom, 1993: Volume flux induced by wind and waves in a saturated sea. *J. Geophys. Res.*, **98**, 4739–4745.
- Weller, R. A., and A. J. Plueddemann, 1996: Observations of the mean vertical structure of the oceanic boundary layer. *J. Geophys. Res.*, **101**, 8789–8806.